Chemical Geology 671 (2025) 122481

Contents lists available at ScienceDirect

Chemical Geology

journal homepage: www.elsevier.com/locate/chemgeo

The effects of carbonate contamination on Ni-Cu-PGE deposit genesis in the Platreef, northern Bushveld Complex: A case study using Niggli numbers

Erin S. Thompson [a,*], David A. Holwell [a], Iain McDonald [b], Marc Reichow [a], Thomas G. Blenkinsop [b], Hannah S.R. Hughes [c], Katie McFall [d], Kate R. Canham [a], Matthew A. Loader [e], Lara Du Preez [f], Kofi Acheampong [f], Andy Lloyd [f]

[a] Centre for Sustainable Resource Extraction, University of Leicester, Leicester, UK
[b] School of Earth and Environmental Sciences, Cardiff University, Cardiff, UK
[c] Camborne School of Mines, University of Exeter, Penryn, UK
[d] Department of Earth Sciences, University College London, Gower Place, London, UK
[e] Anglo American UK, 17 Charterhouse Street, London, UK
[f] Anglo American South Africa, 144 Oxford Road, Rosebank, Johannesburg, South Africa

ARTICLE INFO

Editor: Marco Fiorentini

Keywords:
Bushveld complex
Platreef
Niggli numbers
Contamination
Ni-Cu-PGE

ABSTRACT

Crustal contamination in Ni-Cu-PGE deposit genesis is generally regarded as an essential, or at least highly beneficial, process in triggering sulfide saturation, either through the addition of external sulfur or as a mechanism for increasing oxygen fugacity through the incorporation of volatile-rich lithologies. The Platreef, northern limb of the Bushveld Complex, South Africa, forms one of the world's largest resources of platinum-group elements (PGE), with additional Ni-Cu-Co mineralisation, and represents a unique deposit, intersecting numerous footwall lithologies from the underlying Transvaal Supergroup. In this study, Niggli Numbers, a geochemical tool used to classify rocks on the molecular proportions of their major element geochemistry, are used to examine the degree and styles of contamination in the Platreef at three locations: Tweefontein, Overysel, and a newly drilled deeper section at Sandsloot. The potential impact of these varying contamination styles on PGE-Ni-Cu mineralisation is then discussed. At Tweefontein and Overysel, the highest PGE-Ni-Cu grades are found in largely uncontaminated pyroxenites, exemplified by Niggli *c* values <20. Where carbonate contamination is strong, and Niggli *c* exceeds 30, it is not associated with elevated grades. In contrast, at Sandsloot elevated PGE and Ni grades are strongly associated with carbonate contamination, with Niggli *c* commonly exceeding 20, and Niggli *mg* exceeding 0.8, indicating dolomitic contamination, in the highest-grade horizons. Although other pre-emplacement models may yet explain the elevated grades observed at Sandsloot, there remains a clear correlation between interactions with the Malmani dolomite and elevated Ni-Cu-PGE contents which warrants further investigation.

1. Introduction

Many of the world's Ni-Cu-PGE magmatic sulfide deposits are hosted by mafic intrusions emplaced into sedimentary sequences containing mixtures of evaporites and a wide variety of carbonaceous rocks, including carbonates. Two of the most economically important examples are the Talnakh and Kharealakh deposits of the Norilsk-Talnakh district in Russia, and Jinchuan in China (Lehmann et al., 2007; Sluzhenikin et al., 2023). The role of carbonate contamination in triggering sulfide saturation in mafic/ultramafic magmas has been widely debated, with some arguing it can have a critical control on mineralisation through increases in fO_2, addition of S and volatiles, leading to the production of carbonic fluids and melts (Blanks et al., 2022, Blanks et al., 2019; Lehmann et al., 2007; McFall et al., 2023). Others, however, argue that carbonate contamination plays little no role in the formation of PGE-Ni-Cu mineralisation, with interactions with other contaminants, such as evaporites and sulfide-bearing black shales (Jowitt and Keays, 2011; Naldrett, 1992), playing a larger role, or that contamination of any kind has little impact on the development of mineralisation (Krivolutskaya et al., 2014).

* Corresponding author.
E-mail address: erin.thompson805@gmail.com (E.S. Thompson).

https://doi.org/10.1016/j.chemgeo.2024.122481
Received 8 August 2024; Received in revised form 4 November 2024; Accepted 4 November 2024
Available online 6 November 2024

One of the world's largest PGE-Ni-Cu deposits, the Platreef, located in the northern Bushveld Complex, South Africa. The Platreef extends along >40 km of strike and is intruded into a variety of country rock types (Fig. 1). However, some of the highest-grade mineralisation appears to be located where carbonate units form the surrounding country rock, now preserved as the footwall following the intrusion of the overlaying Main Zone (Pronost et al., 2008). The extent and changing character of the mineralisation along strike, across varying footwall rocks (Fig. 1), enables testing of the hypothesis that different footwall (and inferred hangingwall) rocks might have exercised control. Local contamination from the changing footwall lithologies along strike is known to have created important variations in Platreef mineralogy and geochemistry (Armitage et al., 2002; Barton et al., 1986; Cawthorn et al., 1985; Harris and Chaumba, 2001; Ihlenfeld and Keays, 2011; Keet et al., 2023; Kinnaird et al., 2005; Penniston-Dorland et al., 2008; Pronost et al., 2008; Sharman et al., 2013).

The mafic-ultramafic Rustenburg Layered Suite (RLS) of the Bushveld Complex, South Africa, is host to the largest platinum-group element (PGE) deposits in the world. These include the UG2 chromitite and Merensky Reef of the eastern and western limbs, and the PGE-Ni-Cu Platreef in the northern limb (McDonald and Holwell, 2011). The stratigraphy of the RLS is typically divided into the Upper, Main, Critical, Lower and Marginal Zones, with the Critical Zone (CZ) hosting the majority of the economic PGE-Ni-Cu mineralisation. The Platreef is part of a complex package of rocks with CZ affinities, believed to have formed via the emplacement of a series of magmatic units, or sills (Kinnaird, 2005; Manyeruke et al., 2005; Nyama et al., 2005; Scoon et al., 2020) that were intruded into the Lower Transvaal Supergroup and its Archaean basement prior to the intrusion of the more voluminous Main and Upper Zones (Holwell and Jordaan, 2006). The Platreef differs from the CZ of the wider Bushveld in that layering and cyclic units are less well developed, plagioclase is typically absent as a cumulus phase, and high grade PGE mineralisation is spread over much greater thicknesses, commonly 3–4 g/t 4E (Pt + Pd + Rh + Au), but locally up to 15 g/t, over >10 m (compared to <1 m in the Merensky Reef of the eastern and westerns limbs (Yudovskaya et al., 2011)). Additionally, the Platreef also contains significantly higher base metal contents (Kinnaird et al., 2005; Nex, 2005; Sharman-Harris et al., 2005), and a higher Pd/Pt ratio (>1) than the reefs in the eastern and western limbs, which typically have Pd/Pt ratios <1 (McDonald et al., 2005). This geochemical feature is common to most mineralized and non-mineralized mafic rocks in the northern limb.

Although it is widely accepted that the Platreef magmas are often highly contaminated due to their interactions with the immediately surrounding Transvaal footwall, the importance of this local contamination in triggering sulfide saturation and/or upgrading mineralisation during deposit formation remains debated. This is also the case for several Ni-Cu-PGE deposits globally, such as Norilsk, Kambalda, Voisey's Bay and Nebo-Babel (Keays, 1995; Lightfoot et al., 2012; Naldrett, 2005; Seat et al., 2009), with models often advocating for the importance of the addition of external sulfur, fractional crystallisation, oxygen fugacity variations and even sulfur-poor contaminants.

Early studies in the Platreef argued that following magma emplacement, in-situ contamination alone was enough to trigger sulfide saturation. These models are supported by the presence of metasedimentary xenoliths, crustal S isotope signatures and PGE mineralisation occurring along the base of the Platreef intrusion (Buchanan et al., 1981; Buchanan and Rouse, 1984; Gain and Mostert, 1982; Sharman-Harris et al., 2005; White, 1994). However, the local interactions with the Transvaal footwall following emplacement may have also diluted the metal tenors of the sulfide liquid (Hutchinson and McDonald, 2008; Ihlenfeld and Keays, 2011; Sharman et al., 2013). Furthermore, local contamination signatures are not always evident in the highest-grade intervals, and these intervals are not always located at the base of the Platreef, including at Tweefontein (Nyama et al., 2005), Sandsloot (Penniston-Dorland et al., 2008) and Overysel (Holwell et al., 2007), where mantle-like S isotope signatures have been linked to some of the best mineralized portions. Similar evidence for a lack of local contamination is also reported in the Flatreef at Turfspruit, where the deeper portions of the intrusion display mantle-like S isotope and S/Se signatures, but higher PGE tenors (Keir-Sage et al., 2021). In addition, local contamination from the underlying Transvaal may also have supplied fluids which may redistribute PGEs within the Platreef stratigraphy (Holwell et al., 2006; Mwenze et al., 2019; Pronost et al., 2008), although the scales over which this process may operate are yet to be constrained. Subsequently, the debate over whether contamination from the Transvaal Supergroup is an ore-forming vs ore-modifying process in the Platreef is on-going (Ihlenfeld and Keays, 2011; Penniston-Dorland et al., 2008; Sharman et al., 2013). The application of new, or previously forgotten tools, for assessing the degree and styles of contamination in the Platreef magmas may therefore reveal new insights into its controls on PGE-Ni-Cu mineralisation at scales of 100's-1000's of m of strike; appropriate to an individual resource or mining project.

Niggli Numbers are geochemical tools that can be used to classify rocks based on the molecular proportions of their major element geochemistry (McDonald, 2024; Muthuswami, 1952; Niggli, 1954). The method was first proposed in the 1920s as a simplification of earlier classification tools (Johannsen, 1931), but fell out of fashion from the 1970s onward due to advancements in analytical techniques, promoting trace element and isotopic studies to the forefront of the field of geochemistry. Furthermore, during the time of their introduction, the completion of the necessary calculation steps for Niggli Numbers was time consuming and laborious for large datasets. Today these steps can be easily automated to provide supplementary insights to trace element and isotopic observations (McDonald, 2024).

Benefits of Niggli Numbers include the deliberate exclusion of silica (SiO_2) contents from the calculation of the four primary Niggli terms (*al*, *alk*, *c* and *fm*) (McDonald, 2024). This method helps to avoid the biases created by the closed sum problem, a mathematical problem often associated with compositional geochemical datasets (Buccianti and Grunsky, 2014), and previously combatted by a number of ratio-based approaches such as log-log ratios (Aitchison, 1984; Yang et al., 2019) and Pearce Element Ratios (Pearce, 1968). Niggli Numbers combat the closed sum problem in a simpler fashion by relying on only a portion of the major element data for each calculation, thus accommodating missing elements where the total results are below 100 wt% (McDonald, 2024). Furthermore, the method of combining multiple elements into single terms such as *al* (Al_2O_3 and V_2O_5), *alk* (Na_2O and K_2O), *fm* (FeO, Fe_2O_3, MgO and MnO) and *c* (CaO), works to reduce scatter in the dataset by simplifying the number of degrees of freedom needed to represent minerals. Thus, when plotting data as Niggli Numbers instead of major element oxides alone, the true mineralogical compositions of the dataset are represented more accurately. This method also removes the need to account for the oxidation state of iron (as Fe^{2+} and Fe^{3+} are combined in a single term) and the volatile content of the rock. A full explanation of the calculation, uses and benefits of Niggli Numbers is provided by McDonald (2024).

They can also be readily applied to all rock types, making them extremely useful in the context of the Platreef, where magmatic packages are often interspaced with a range of rock types, including metasedimentary xenoliths and surrounding highly altered and contaminated hybrid lithologies (Kinnaird et al., 2005; Maier et al., 2008; McDonald and Holwell, 2011). However, they have received limited use in the Bushveld Complex, having only been applied in one previous study to examine hybrid footwall samples from the eastern limb (Toens, 1954).

McDonald (2024) revisited Niggli Numbers and outlined their key advantages for reducing the complexity of large datasets, and tracing contamination, hydrothermal alteration and chemostratigraphy in several settings, including the Bushveld Complex. In this study we aim to highlight the effectiveness of Niggli Numbers in tracking carbonate contamination, building on the initial analysis presented in McDonald (2024). We also aim to examine the link between contamination from

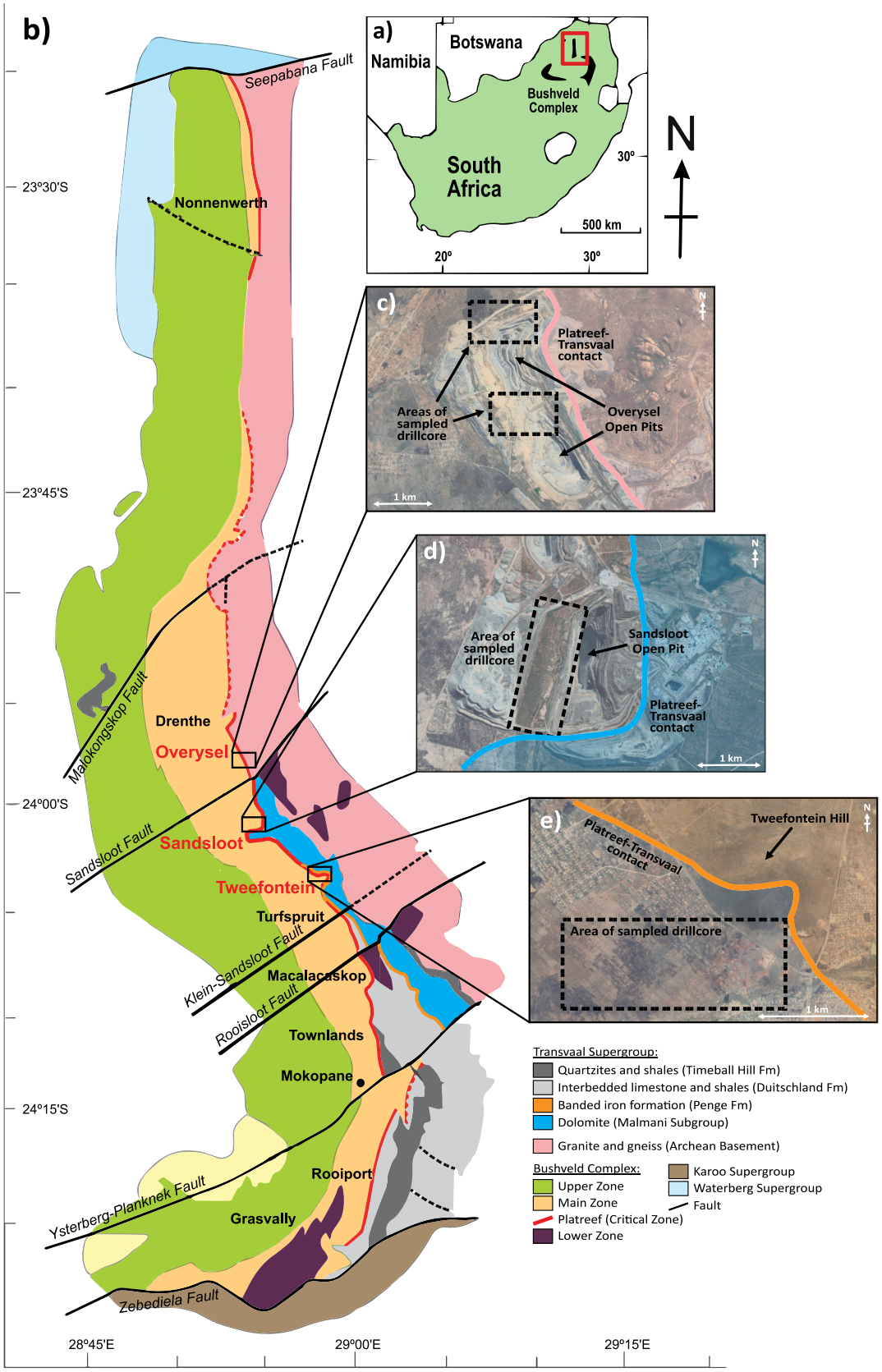

Fig. 1. a) Location of the Bushveld Complex in South Africa. The northern limb is highlighted in red. b) Geological map of the northern limb of the Bushveld Complex. Study locations labelled in red (modified after Keet et al., 2023); c-e) Satellite image showing the locations of sampled drill core from Overysel, Sandsloot and Tweefontein respectively. (For interpretation of the references to colour in this figure legend, the reader is referred to the web version of this article.)

the various Transvaal footwall lithologies, highlighted by the Niggli Numbers, and PGE-Ni-Cu mineralisation in the Platreef along the northern limb. Three locations along the strike of the northern limb (Fig. 1) with differing footwall lithologies are examined, Tweefontein (shale, carbonate and banded iron formation (BIF) footwall), Sandsloot (dolomite footwall) and Overysel (granite-gneiss footwall). Both the occurrence and magnitude of mineralisation is proposed to potentially be controlled by the differing footwall contaminants, however other models including pre-emplacement processes are also possible.

2. Geology of the Platreef

The Platreef comprises a complex zone of igneous and hybrid lithological units, which lie, from south to north, on progressively older units of the Transvaal Supergroup and the Archean Basement footwall, and beneath the Main Zone of the RLS (Kinnaird and McDonald, 2005). The igneous units are composed of (feldspathic-) pyroxenites, gabbronorites, norites, harzburgites and peridotites, with orthopyroxene being the most common cumulus phase, but increasing cumulus clinopyroxene, olivine and interstitial phlogopite in contaminated zones (Cawthorn et al., 1985; Ihlenfeld and Keays, 2011). Xenolith rafts, sometimes up to 1500 m wide and 100 m thick, are common along the entire strike of the northern limb, and often produce halos of highly altered lithologies, and more proximal recrystallised hornfels and parapyroxenite (metasomatized and contaminated serpentinised (clino-) pyroxenites and calcsilicate hybrid lithologies) packages (Kinnaird et al., 2005).

As the Platreef transgresses down the Transvaal stratigraphy from south to north, it first contacts the quartzites and shales of the Silverton and Timeball Hill Formations on the farms Townlands to Macalacaskop, followed by the calcareous shales of the Duitschland Formation from Turfspruit to Tweefontein, the banded iron formation (BIF) of the Penge Formation at Tweefontein and the dolomites of the Malmani Supergroup from north Tweefontein and Sandsloot to Zwartfontein. From Zwartfontein onwards, the Platreef sits on Archean granites and gneisses (Fig. 1) (McDonald and Holwell, 2011). This study focuses on the variations in footwall controls from Tweefontein northwards.

At Tweefontein, the Platreef forms an approximately 100–500 m thick package, dominated by pyroxenites with minor (gabbro-) norites (White, 1994). At Tweefontein Hill, the Platreef intruded into a footwall trough structure, allowed the pooling of the sulfide liquid and the formation of massive to semi-massive sulfide mineralisation (Nex, 2005). Nyama et al. (2005) used Mg# and Fe/Ti ratios to divide the Platreef at Tweefontein into at least three different magmatic packages at this location. Closer to the Penge footwall, the Platreef has been locally contaminated, producing a distinctive Fe-enrichment towards the footwall contact (Buchanan et al., 1981; Ihlenfeld and Keays, 2011), however this has also been noted towards the top of the Platreef sometimes (Nyama et al., 2005), and significant carbonate contamination has also been identified in some units via elevated CaO/Al_2O_3 and CaO/MgO values (Ihlenfeld and Keays, 2011; McCutcheon, 2012).

At Sandsloot, the Platreef overlies the dolomitic Malmani Subgroup, which also contains anhydrite (Buchanan et al., 1981). Its shallowest exposures in the Mogalakwena open pit (Fig. 1c) have been examined by several authors (Armitage et al., 2002; Harris and Chaumba, 2001; Holwell, 2006; Holwell et al., 2005; McDonald et al., 2005) and are characterised by a series of variably serpentinised (feldspathic-) pyroxenites, with basal clinopyroxenites and calcsilicate hornfels forming the footwall. Extensive carbonate contamination and hydrothermal alteration is often evident within the magmatic units. More recent work, including the drilling presented in this study, has revealed thicker pyroxenitic sequences present in the deeper portions of the Platreef at Sandsoot.

The farm Overysel sits in the northern sector of the northern limb, with the Platreef overlying the Archean basement (Cawthorn et al., 1985; Holwell and McDonald, 2006). Thus, signatures of local contamination and alteration are typically less prevalent, with the primary magmatic assemblage of alternating (feldspathic-) pyroxenites being better preserved. Minor quartzo-feldspathic pyroxenites at the base of the succession indicate local granitic footwall contamination (Cawthorn et al., 1985), and calcsilicate xenoliths, likely sourced from the pre-Main Zone hanging wall, and their associated carbonate contamination signatures, can also be present (Holwell and McDonald, 2006).

3. Methods

A selection of drillholes from the farms Tweefontein, Sandsloot and Overysel were chosen to examine to the influence of contamination from the Transvaal and Archean country rocks on PGE-Ni-Cu mineralisation (Fig. 2). At Tweefontein, data from five drillholes in the Tweefontein Hill area (RTN020, RTN021, TN304, −303 and − 287) were examined, three drillholes at Overysel (OY1050, −923 and − 894), and six drillholes from Sandsloot (SSAA019, −029, −034, −043, −056 and − 062). The drillholes from Sandsloot are part of a recent drilling programme which samples the deeper Platreef succession, down dip of the exposures in the Sandsloot open it (Fig. 1c).

Lithological core logging results for the selected drillholes from Overysel and Tweefontein were provided by Anglo American. Logging of the selected drillholes from Sandsloot was conducted by the authors. Bulk rock geochemistry for whole metre-intervals of half core from drillholes from Tweefontein were collected via ICP-OES for major elements, and ICP-MS for trace elements, including Ni and Cu, by Bureau Veritas Minerals on behalf of Anglo American. Platinum and Pd grades were collected via lead collection fire assay fusion followed by ICP-MS. Whole metre-intervals of half core from drillholes from Sandsloot and Overysel were analysed for major elements via XRF on borate fusion beads by SGS South Africa on behalf of Anglo American. Pressed pellets were used for XRF for the collection of Cu, Ni and Co concentrations. Additionally, Pt and Pd grades were collected via lead collection fire assay fusion followed by ICP-OES.

The data supplied by Anglo American was supplemented by further analysis of 80 quarter core samples from Tweefontein and Sandsloot via XRF at the University of Leicester. The purpose of this analysis was to provide an external quality check on the data supplied by Anglo American only, and these results are not used in the Niggli Number analysis. Each sample, ranging from 20 to 40 cm in interval width depending on grainsize, was crushed with a hardened steel press, and milled in an agate planetary ball mill. After each run, the apparatus was decontaminated and sterilised using water and industrial methylated spirit. XRF analysis was conducted on a PANanlytical Axios Advanced XRF spectrometer, operating with PANanlytical SuperQ software. Major elements were determined via analysis on fusion beads prepared using a lithium tetraborate flux followed by XRF. The standards run were BE-N, GH, JA-1, JGb-1, PCC-1 and RGM-1, and all corresponded well with accepted values (see Appendix 2).

These repeat results were in good agreement with the previous analyses conducted by Anglo American, with relative standard deviation (RSD) between samples typically <15 %, and below 10 % in the least variable intervals. It is important to note that each data point supplied by Anglo American is an average composition over a whole metre-interval, including quartzo-feldspathic veins and post-Bushveld granitic intrusions, whereas the collected samples have been selected to exclude xenoliths/granitic intrusions/quartzo-feldspathic veins and therefore have much smaller interval lengths. Thus, some intervals display larger variations in RSD between the Leicester and Anglo American datasets, however the overall correlation between these two datasets remains very strong (R^2 always >0.87 but typically >0.97 for most major elements). Comparisons between the intervals analysed by both Anglo American and Leicester, including graphical representations, are found in Appendix 2. Due to the commercially sensitive nature of the Anglo American dataset, this cannot be made available in full.

The magmatic units in the Platreef are commonly interspaced with

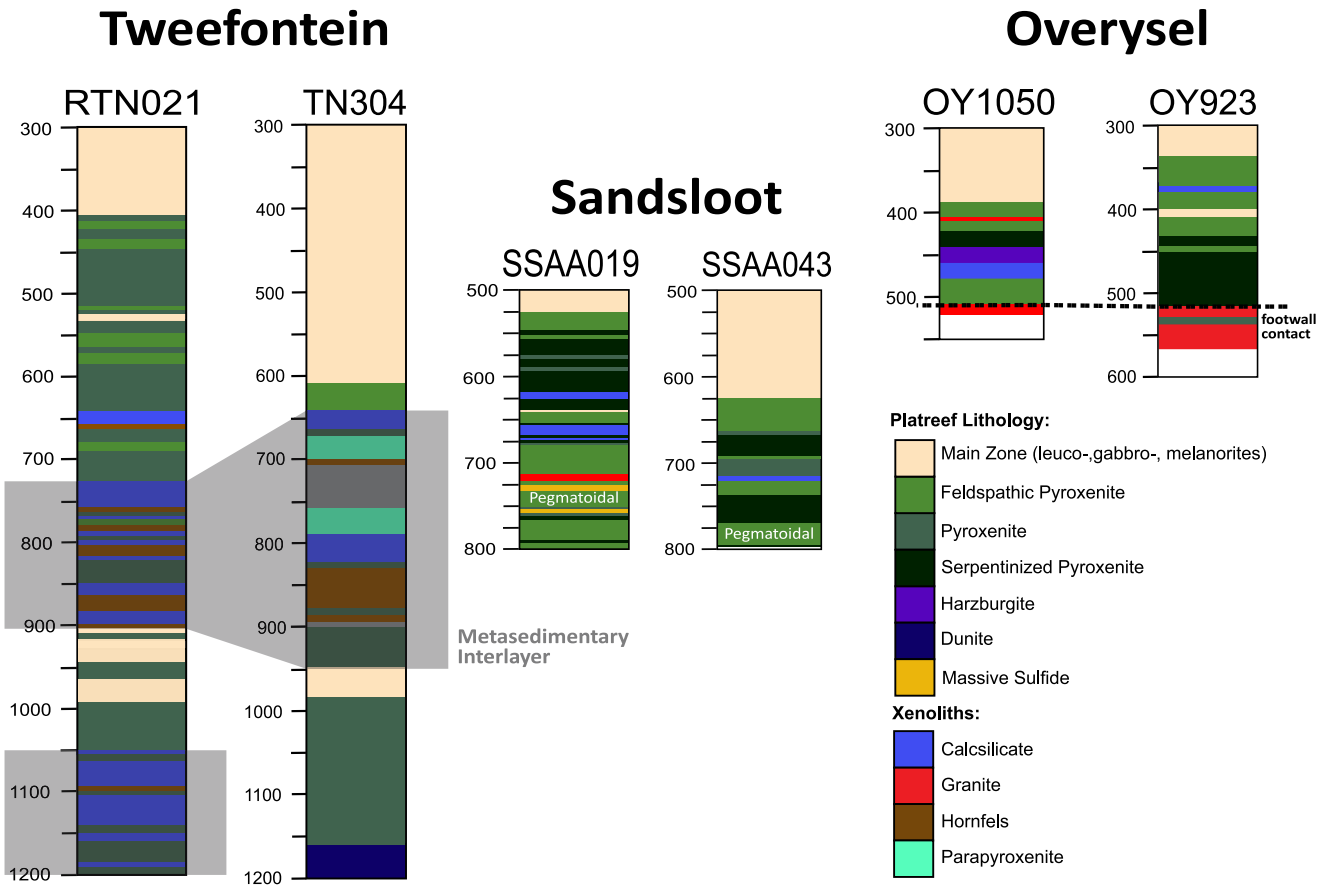

Fig. 2. Lithology logs from selected representative drillholes from Tweefontein, Sandsloot and Overysel. Thick metasedimentary interlayers which separate the magmatic packages in the Platreef at Tweefontein are highlighted in grey, and are excluded from the current study. The logging of the Sandsloot drillholes was conducted by the authors, and at Tweefontein and Overysel was conducted by Anglo American. See the Appendices (Fig. A1–3) for logs for all drillholes included in this study.

large rafts of metasedimentary interlayers as discussed above. In this study this is particularly the case at Tweefontein, with xenolith rafts of metasediments, calcsilicates and hornfels up to 200 m thickness in the selected drillholes (Fig. 2). As this study is focussed on the contamination and controls on PGE-Ni-Cu mineralisation within the magmatic units, these zones have been omitted from the analysis.

The method for calculating Niggli Numbers is outlined fully in McDonald (2024), Niggli (1954) and Muthuswami (1952), including spreadsheets to automate the calculations of both primary and secondary Niggli Numbers, and Niggli sums or ratios. In this study, the 'Niggli Modified' scheme proposed by McDonald (2024) is applied, where Cr is combined with Mg, Fe, Mn and Ni in the *fm* term, as opposed to with Al in the classical scheme, reflecting the natural association between Cr and Fe in chromite-bearing pyroxenites, which is more appropriate in mafic-ultramafic systems such as the RLS.

Compositions for key minerals in the northern limb, country rock lithologies, and data from the Upper Critical Zone (UCZ) of the eastern and western limbs of the Bushveld Complex, are shown on the three Niggli diagrams which are used in this study: (*al-alk*) versus *c*, (*al-fm*) + (*c-alk*) versus *si and mg* versus *si* (Fig. 3). The UCZ data is employed as a benchmark to compare against the Platreef data presented in this study, however the key aim of this paper is to examine the role of contamination on PGE-Ni-Cu in the northern limb. The sources of the compositions for the various rocks and minerals are listed fully, alongside full explanations for each diagram and Niggli term, in McDonald (2024). These Niggli plots are used to access the changing mineralogy, most commonly linked to the style and degree of contamination, in the Platreef magmas at each study location.

4. Results

Niggli (*al-alk*) vs *c* (Fig. 4) is used to access carbonate vs shale contamination trajectories, as both lithologies are present within the Duitschland and Malmani Transvaal footwall. The size of all Platreef data symbols are scaled to reflect Pt (Fig. 4a, d, g) and Ni (Fig. 4b, e, h) grades. Only Pt and Ni grades are reported here (Fig. 4), but analysis has shown that Pd follows the same trends at Pt at all study locations, as does Cu with Ni grades. The results for Pd and Cu are presented in the Appendices (Fig. A4-A6). The field for carbonate skarn (Fig. 3) minerals including diopside, grossular garnet and epidote is also indicated. Downhole plots for example drillholes from each location (RTN021, SSAA019 and OY1050) are also presented (Fig. 4c, f, i).

When comparing the data from the Platreef to the UCZ of the eastern and western limbs of the Bushveld Complex, there are clear differences, the most striking of which are the lack of contamination in the UCZ compared to the Platreef, where the UCZ data fall close to the plagioclase-OPX mixing line, and the conspicuous lack of plagioclase in the Platreef (Fig. 4) compared to the UCZ. This trend is present in all three Platreef locations, with the least contaminated portions showing *al-alk* compositions <10, indicating peridotite to pyroxenitic compositions, whereas the UCZ contains (*al-alk)* values from 5 to 40, indicating compositions from pyroxenite through to leucogabbronorite.

When examining local contamination signatures in the Platreef itself, at Tweefontein, where the Duitschland Fm and Penge BIF form the footwall from south to north, there is little evidence for significant local contamination from either carbonate or shale sources (Fig. 4a-b) in terms of deviation from the plagioclase-OPX mixing line. There is some

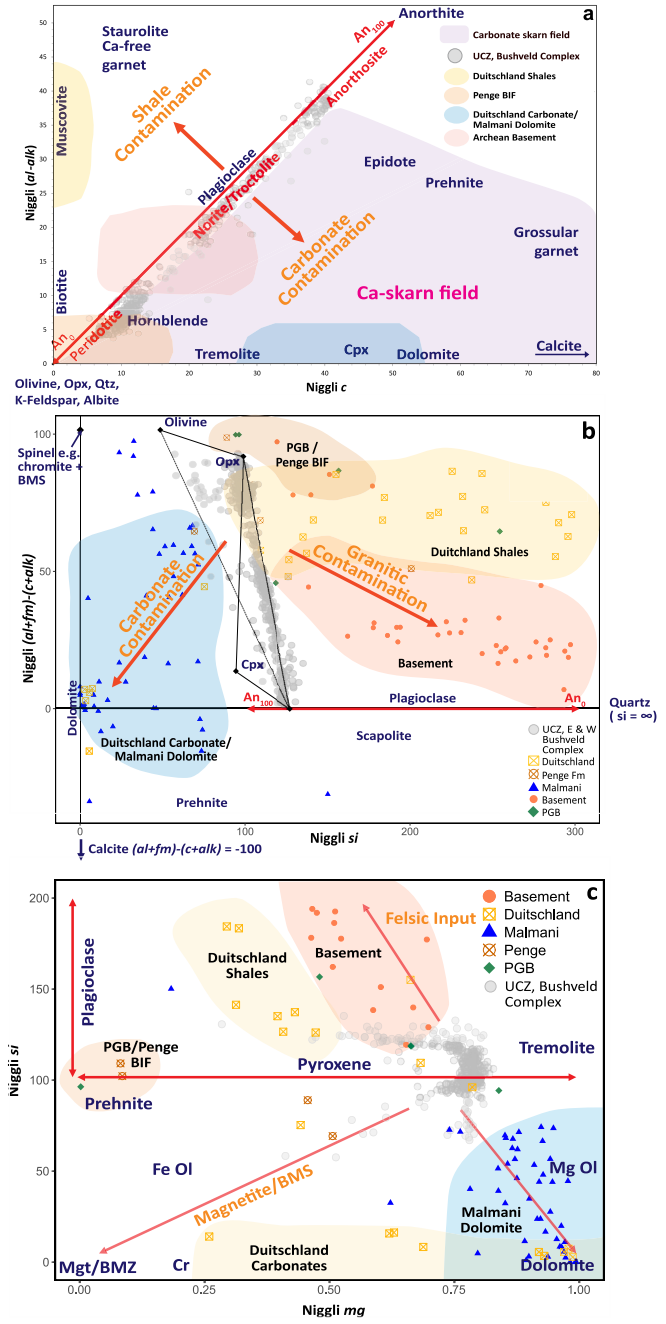

Fig. 3. Mineral compositions for common Bushveld minerals, footwall and the UCZ of the western and eastern limbs in the Niggli plots used in this study, modified after McDonald (2024); a) Niggli *(al-alk)* vs *c*. Uncontaminated igneous lithologies plot along the red line (gradient m = 1), whereas sedimentary lithologies vector in the opposite direction. Vectors for shale and carbonate contamination, Transvaal and Archean footwall and carbonate skarns are labelled; b) Niggli *(al + fm)-(c + alk)* vs *si*. Typical Bushveld minerals are labelled, as well fields for the Transvaal and Archean footwall lithologies and vectors for carbonate and granitic contamination. An_{80} composition in b is used to reflect the average plagioclase content of the UCZ after McDonald (2024); c) Niggli *mg* vs *si*. Footwall data from Stephenson (2018), McDonald (2024) and references therein. BMS = Base metal sulfides, Mgt = Magnetite. See McDonald (2024) for references for UCZ data. (For interpretation of the references to colour in this figure legend, the reader is referred to the web version of this article.)

overlap with the field for the Penge BIF, but this is difficult to distinguish from a typical uncontaminated igneous trend, and data from the plagioclase-poor portions of the UCZ, in this diagram. The vast majority of Platreef data at Tweefontein plots with Niggli *c* values of 5–20, slightly elevated compared to the uncontaminated igneous vector (red arrow) indicating slight carbonate contamination, likely due to interactions with the calcsilicate and metasedimentary xenolith rafts which sit between the magmatic units at this location (Fig. 2). Some samples do exhibit Niggli *c* values >30 indicating stronger carbonate contamination, however this is not linked to any increased in Pt or Ni grades, and actually shows decreased grades compared to the less contaminated sections of other Tweefontein drillholes. The highest Pt and Ni grades are not linked to strong local contamination, instead indicating that PGE-Ni-Cu mineralisation at Tweefontein is not controlled by country rock interactions. Similar results are reported for Overysel, where the Archean basement forms the footwall, but calcsilicate xenoliths are also present and dolomite was likely to have formed much of the hangingwall at the time of intrusion. There is little deviation above Niggli *c* values of >20 and *(al-alk)* values of <10 (Fig. 4g-h). The highest Pt and Ni grades are found in this relatively uncontaminated zone, with the bubble sizes for both Pt and Ni contents decreasing with elevated Niggli *c* and *(al-alk)* values.

In stark contrast, the results from the deeper Platreef at Sandsloot show a different trend from the locations to the north and south (Fig. 4d-e). Here there is a distinct, and strong trend towards carbonate contamination, with the vast majority of the data from all drillholes reporting Niggli *c* values >20, well into the carbonate skarn field (McDonald, 2024). In the case of Pt grades, bubble size increases with increasing Niggli *c*, and thus carbonate contamination (Fig. 4d). It is also clear that the Pt grades present within the Platreef at Sandsloot are significantly elevated compared to those at Tweefontein and Overysel (Fig. 4d). Several intervals with elevated Ni grades are also strongly associated with carbonate contamination, and also contain elevated *(al-alk)* contents compared to the highest Pt intervals (Fig. 4d-e). The intervals with the highest Ni contents plot closer to the origin, and are associated with the zones of massive to semi-massive sulfide mineralisation present intermediately at the base of the Platreef at Sandsloot (and shown in drillhole SSAA019 in Fig. 2). As a result, these intervals are lower in both *c* and *al-alk* values. Nickel grades at Sandsloot are also significantly elevated compared to those of Tweefontein and Overysel (Fig. 4).

The Niggli *(al + fm)-(c + alk)* vs *si* (Fig. 5) diagram offers additional advantages in that it can be used to investigate contamination signatures from specific Transvaal, Archean and other country rocks (Fig. 3), including the Pietersburg Greenstone Belt (PGB), which sits beneath the Transvaal Supergroup to the west of the northern limb (de Wit, 1991; Stephenson, 2018), and thus may have interacted with the Platreef magmas at depth. The diagram can also be used demonstrate chromite and base metal sulfide (BMS) enrichment, as the pure compositions of these minerals will plot at 0 *si* and 100 *(al + fm)-(c + alk)* (Fig. 5). Olivine and orthopyroxene compositions can also be distinguished in this plot, unlike in *al-alk* vs *c*, where both the Niggli *c* compositions largely overlap (Fig. 3).

Similarly to the *(al-alk)* versus *c* diagram, uncontaminated Platreef data are typically clustered around the orthopyroxene endmember composition, indicating pyroxenitic lithologies are dominant, as opposed to the UCZ, where the data ranges from >90 to 0 in *(al + fm)-(c + alk)*, representing a wide range of plagioclase modal abundances in rocks represented by a mix of pyroxenites, to norites and anorthosites. At Tweefontein and Overysel, similar to in *(al-alk)* vs *c* Niggli space, there is little evidence of considerable local contamination. Most of the data plot within the mineral field for orthopyroxene, plagioclase, olivine and clinopyroxene (Fig. 5a-b, 5g-h), with the vast majority clustering around orthopyroxene, as expected for relatively uncontaminated feldspathic orthopyroxenites. Several samples from Tweefontein contain higher *(al + fm)-(c + alk)* values, and plot within the Penge/PGB contaminated

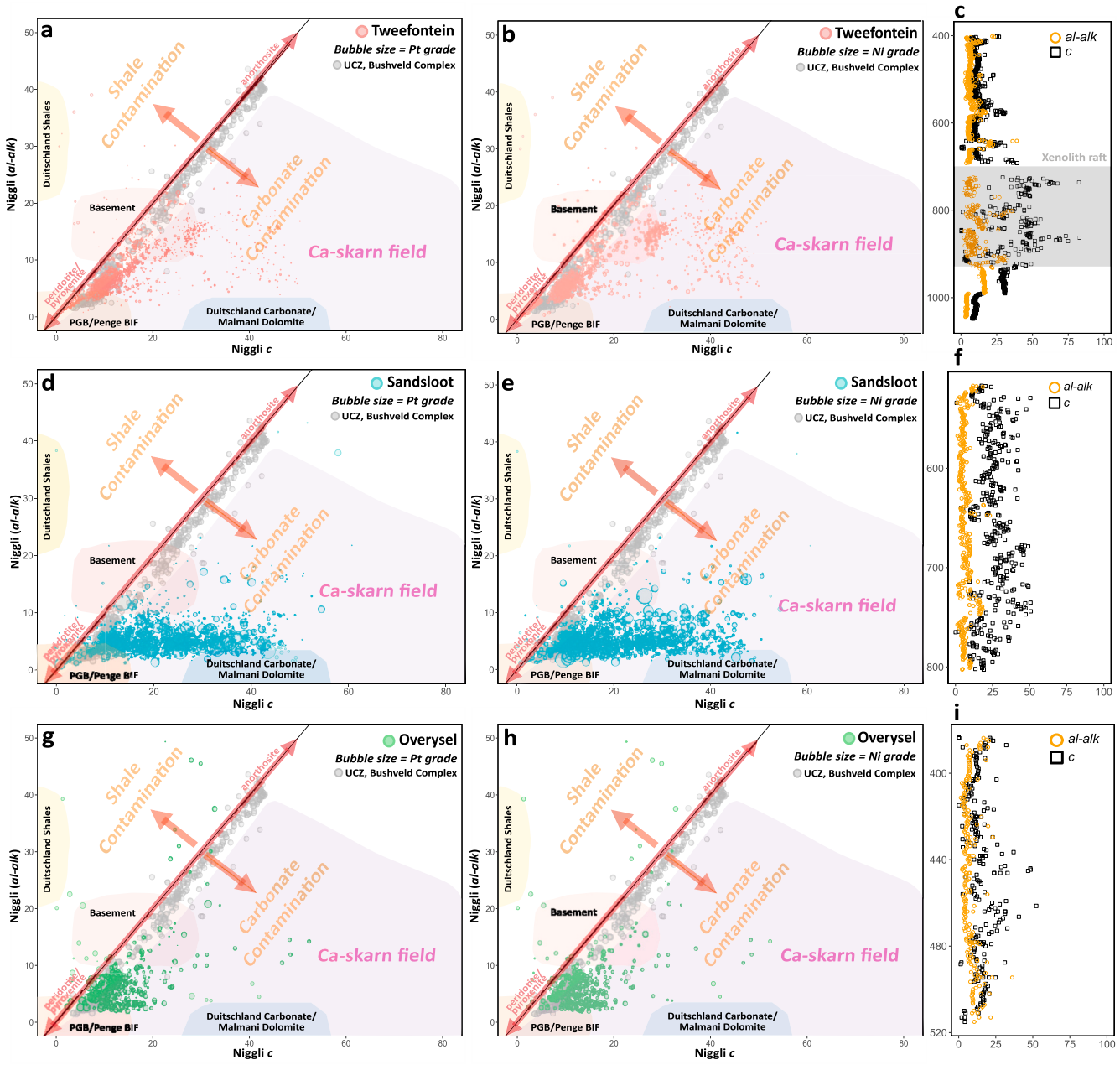

Fig. 4. Niggli *(al-alk)* vs *c* bubble plots for the Platreef at each study locations, the UCZ of the western and eastern limbs and downhole plots for example drillholes (modified after McDonald, 2024). The size of the bubbles for the Platreef data correspond to either Pt (ppm) or Ni (wt%) grades. Vectors for shale and carbonate contamination, carbonate skarns and fields for Transvaal and Archean footwall lithologies are annotated (modified after Fig. 3); a) Pt bubble plot for Tweefontein; b) Ni bubble plot for Tweefontein. No Ni data was available for drillholes TN303 or TN304; c) Downhole Niggli *c* and *(al-alk)* for RTN021; d) Pt bubble plot for Sandsloot; e) Ni bubble plot for Sandsloot; f) Downhole Niggli *c* and *(al-alk)* for SSAAA019; h) Pt bubble plot for Overysel; h) Ni bubble plot for Overysel; i) Downhole Niggli *c* and *(al-alk)* for OY1050. See Fig. 2 for drillhole lithology logs. A xenolith raft in RTN021 (shaded grey) is not shown in the bubble plots.

field, reflecting local BIF contamination and some display stronger carbonate contamination signatures, producing lower *(al + fm)-(c + alk)* values (Fig. 5a-b) and clustering around clinopyroxene compositions. This is accompanied by decreasing Pt and Ni grades, as the highest grades for both Pt and Ni at Tweefontein and Overysel are clustered around orthopyroxene compositions. An enrichment in Cr in several of the Overysel samples, particularly from OY1050, produces a trend towards 0 *si* and 100 *(al + fm)-(c + alk)* (Fig. 5g) due to the chromitite stingers present in some of the Overysel drillholes (Fig. 2). There is some evidence for slight carbonate and granitic contamination at Overysel (Fig. 5g-i), however, this increased local contamination is not associated with increased grades here. Although the data which plots to the right of the mineral field at Overysel often appear to fall in the Duitschland Shales contamination field, as the Archean basement granite forms the footwall at Overysel, and *si* values increase towards this contact (Fig. 5i), this trend is interpreted as a trend vectoring away from orthopyroxene cluster towards the Basement field due to granitic contamination (Fig. 5g).

At Sandsloot, three trends are observed, two of which correspond to enhanced Pt or Ni grades (Fig. 5d-e). The intervals with both the lowest Pt and Ni grades cluster below the orthopyroxene composition, reflecting a relatively uncontaminated pyroxenite. The highest Pt grades form a trend between olivine and clinopyroxene compositions (Fig. 5d), as they contain lower si values than at Tweefontein, Overysel and the UCZ,

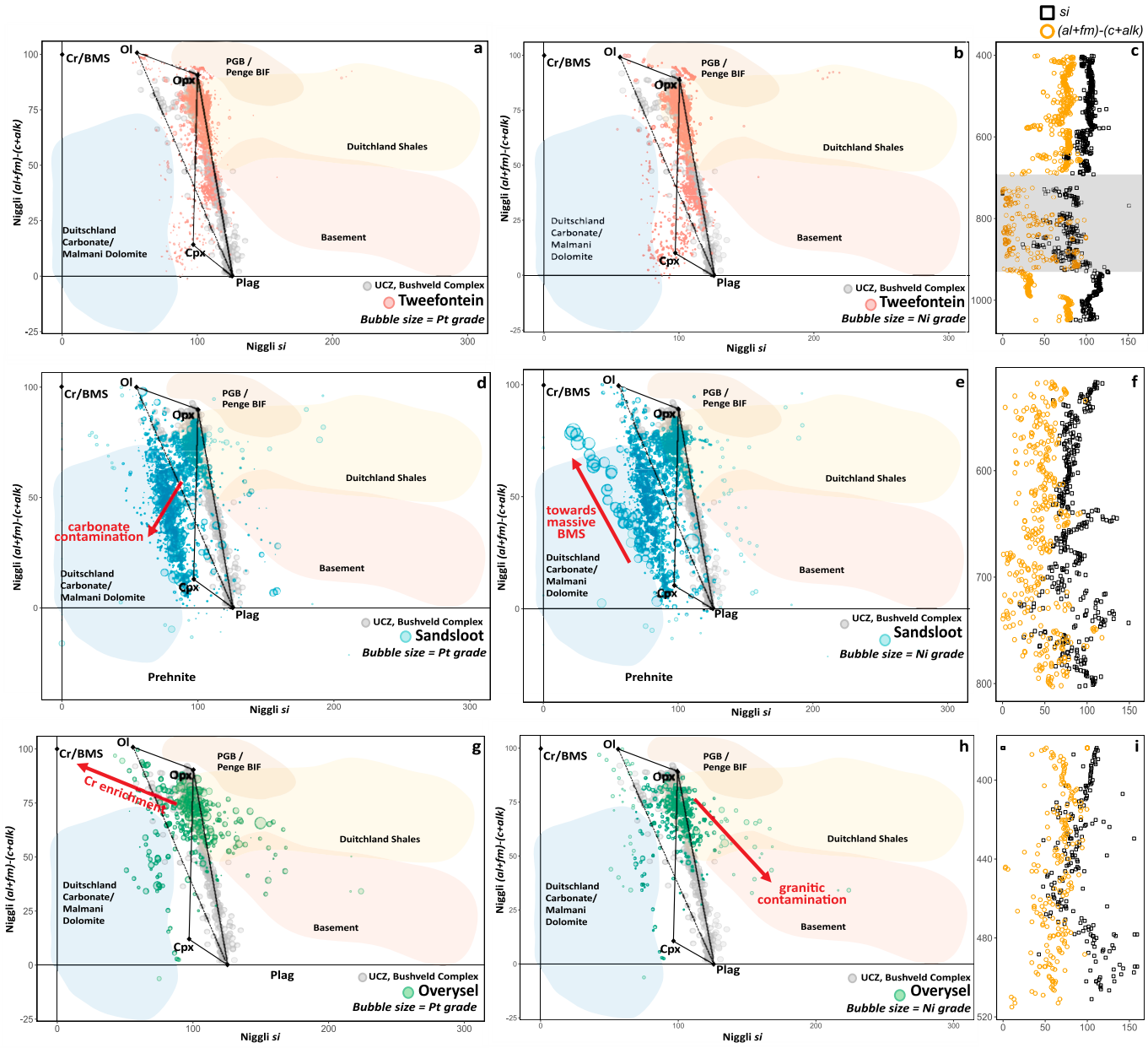

Fig. 5. Niggli *(al + fm)-(c + alk)* vs *si* bubble plots for the Platreef at each study location, the UCZ of the western and eastern limbs, Transvaal footwall lithologies and downhole plots for example drillholes. Bubble sizes for the Platreef data are scaled to either Pt (ppm) or Ni (wt%) grades; a-b) Tweefontein Pt and Ni grades respectively. Magmatic units only. No Ni data was available for drillholes TN303 or TN304; c) Downhole Niggli *si* and *(al + fm)-(c + alk)* plot for RTN021; d-e) Sandsloot Pt and Ni grades respectively; f) Downhole Niggli *si* and *(al + fm)-(c + alk)* plot for SSAA019; g-h) Overysel Pt and Ni grades respectively. i) Downhole Niggli *si* and *(al + fm)-(c + alk)* plot for OY1050. An_{80} composition for UCZ plagioclase chosen after McDonald (2024). For lithology logs see Fig. 2. A xenolith raft in RTN021 (shaded grey) is not shown in the bubble plots.

and thus plot much closer to the carbonate contamination field. The highest Ni grades are shifted towards even lower *si* values, forming a trend between clinopyroxene and chromite or massive BMS compositions (Fig. 5e), with the latter being evident in the lower portions of the Platreef at Sandsloot and associated with these Ni-rich samples (Fig. 2, Fig. 5f). Several samples also trend towards prehnite. Although some samples do plot within the Duitschland shale contamination field, these are not associated with elevated grades, and very few of the data plot within either the Basement or Penge/PGB fields at Sandsloot.

Strong carbonate contamination is clearly evident in the Platreef, most notably at Sandsloot (Figs. 4 and 5). Examining the *mg* Niggli term can differentiate carbonate and dolomitic contamination signatures (Fig. 6) from the Transvaal country rocks. Firstly, when comparing the Platreef to the UCZ, the majority of the Platreef data displays lower *si* values and higher *mg* values, compared to the UCZ due to the lower abundance of plagioclase. The data from Tweefontein and Overysel does overlap with portions of the UCZ, whereas the majority of the Platreef at Sandsloot is offset from the UCZ (Fig. 6).

At Tweefontein and Overysel, as shown above (Figs. 4 and 5), there is little evidence of local contamination with the bulk of the Platreef data clustering around *mg* 0.75 and *si* 100. Some intervals at both locations do trend towards the carbonate and dolomite contamination fields, but are not associated with increased in Ni-Cu-PGE grades. A few samples at Overysel also overlap with the Archean Basement field (Fig. 6g-h), indicating minor local granitic contamination, and at Tweefontein several low-grade intervals display lower *mg* values, trending towards

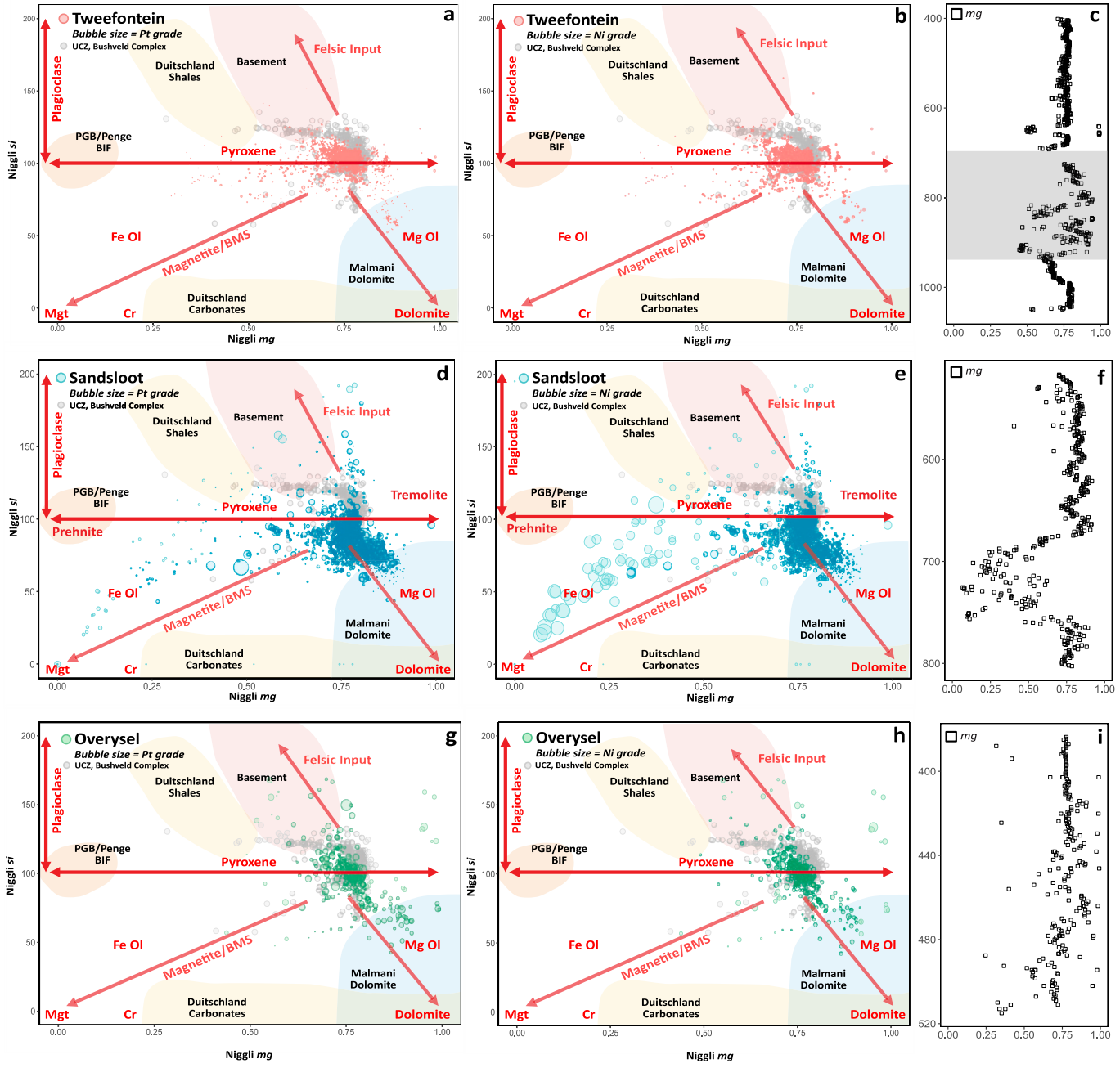

Fig. 6. Niggli mg vs si bubble plots for the Platreef at each study location, the UCZ of the western and eastern limbs, Transvaal footwall lithologies (after McDonald, 2024) and downhole plots for example drillholes. Bubble sizes for the Platreef data are scaled to either Pt (ppm) or Ni (wt%) grades; a-b) Tweefontein Pt and Ni grades respectively. Magmatic units only. No Ni data was available for drillholes TN303 or TN304; c) Downhole Niggli mg for RTN021; d-e) Sandsloot Pt and Ni grades respectively; f) Downhole Niggli mg for SSAA019; g-h) Overysel Pt and Ni grades respectively; i) Downhole Niggli mg for OY1050. For lithology logs see Fig. 2. A xenolith raft in RTN021 (shaded grey) is not shown in the bubble plots.

the BIF contamination field (Fig. 6a-b).

In contrast, the Platreef at Sandsloot is clearly offset from the pyroxene composition line (Fig. 6d-e), displaying both lower *si*, and higher *mg* values with the majority of the data trend towards the dolomite contamination field. The intervals with the higher Pt grades are found within this cluster trending towards dolomite (Fig. 6d). The highest Ni grades, associated with the massive sulfide mineralisation identified at the base of the Platreef at Sandsloot, trend towards the origin, with *mg* values typically below 0.5 (Fig. 6e-f). The slightly elevated *si* values in these intervals compared to the typical BMS/magnetite trend arrow reflects the presence of prehnite, also shown in Figure 5, which is abundant as an alteration product of plagioclase in this portion of the Platreef at Sandsloot.

5. Discussion

This study builds on a brief case study presented by McDonald (2024) which alluded to a correlation between carbonate contamination and elevated PGE grades in the northern limb of the Bushveld Complex. The Niggli *c* term is shown to be a very useful tool for identifying carbonate contamination (Fig. 4), and both the *mg* and *si* terms are useful for distinguishing specifically dolomite contamination from carbonate contamination, and identifying zones of massive sulfide (Figs. 5 and 6). Utilising Niggli Numbers to access the potential influence of

contamination on PGE-Ni-Cu mineralisation in the Platreef across three very different footwall types reveals two distinct trends when comparing the farms Tweefontein and Overysel to Sandsloot. At Tweefontein and Overysel, local contamination signatures from the underlying Transvaal Supergroup and Archean Basement are less prevalent compared to Sandsloot, and the horizons which do show evidence of elevated carbonate or granitic contamination are not associated with elevated PGE or Ni contents (Figs. 4 and 5). At Sandsloot however, much of the Platreef sequence is characterised by significant carbonate contamination, with Niggli *c* values typically >20 and low (*al-alk*)/*c* ratios (Fig. 4). Additionally, PGE-Ni-Cu mineralisation is associated with carbonate, and particularly dolomitic, contamination at Sandsloot, with grades significantly elevated compared to those at Tweefontein and Overysel. The impacts of these varying contamination signatures in the Platreef along the strike of the northern limb, and whether or not dolomitic contamination may be linked directly to increased Ni-Cu-PGE mineralisation at Sandsloot, are discussed below.

5.1. Evidence of local contamination in the Platreef

Comparisons between the Platreef, northern limb of the Bushveld Complex, and the UCZ of the eastern and western limbs in Niggli space (Figs. 4–6) support the widely accepted belief that the Platreef has undergone significantly higher degrees of local contamination compared to the UCZ (Buchanan and Rouse, 1984; Harris and Chaumba, 2001; Ihlenfeld and Keays, 2011; McDonald, 2024; Pronost et al., 2008). Furthermore, the UCZ consistently shows higher *si* and (*al-alk)* values compared to the Platreef, indicating a higher plagioclase content in the UCZ, and a wider range of primary lithologies present. This is consistent with past studies noting the general lack of cumulus plagioclase in the Platreef compared to the UCZ, with orthopyroxene mesocumulates and orthocumulates dominated the Platreef, whereas norites and anorthosites are common at the top of the chromitite-pyroxenite-norite cyclic units which form the UCZ (Eales and Cawthorn, 1996).

The degree of local contamination is known to vary along the strike of the northern limb, with changes in the footwall architecture (Kinnaird et al., 2005) and reactivity of the country rock lithologies proposed as major controlling factors (e.g. Ihlenfeld and Keays, 2011; McDonald et al., 2005). The dolomites of the Malmani Subgroup, and carbonaceous shales and limestones of the Duitschland Formation, are thought to be more chemically reactive compared to the relatively inert granites of the Archean Basement, and the BIFs and iron-rich shales of the Penge Formation (Harris and Chaumba, 2001; Ihlenfeld and Keays, 2011; McDonald and Holwell, 2011). This increased reactivity enhances interactions with the intruding Platreef magmas, thus elevating their CaO and MgO contents (De Waal, 1977; Manyeruke et al., 2005), and thus increasing Niggli *c* and *mg* values, as observed at Sandsloot (Figs. 4 and 6). These results correlate with past studies using both stable and radiogenic isotopes which identify significant carbonate, and dolomitic, contamination in the Platreef at Sandsloot, with less pervasive contamination from carbonate and granitic sources at Turfspruit and Overysel respectively (Cawthorn et al., 1985; Harris and Chaumba, 2001; Pronost et al., 2008).

As increases in CaO and MgO subsequently lower SiO_2 contents, a corresponding decrease in Niggli *si* values is also observed (Fig. 6). Increasing Niggli *c* values also decreases the *(al + fm)-(c + alk)* function (Fig. 5). As the Platreef at Tweefontein Hill and Overysel sits above the Penge BIFs and Duitschland Formation, and the Archean Basement, respectively, the reduced reactivity of these units may supress local contamination in these areas. As a result, elevated Niggli *c* and reduced Niggli *si* values in the context of carbonate contamination, and increased Niggli *si* values in the context of granitic contamination, are only present in horizons either adjacent to xenoliths or the footwall at these locations (Fig. 5i), as opposed to being ubiquitous with the majority of the magmatic sequence, as demonstrated at Sandsloot. In *mg* vs *si* space, several intervals at Tweefontein do also trend towards the Penge BIF field (Fig. 6a-b), alluding to minor iron-rich contamination above the footwall in some locations, as has been reported in past studies in the area (Nyama et al., 2005).

The effect of carbonate contamination at Sandsloot appears to be profound, producing highly distinctive Niggli Number characteristics (Figs. 4–6) and mineral assemblages, containing mixtures of olivine and clinopyroxene (Figs. 4 and 5). Conversely, the Platreef at Tweefontein and Overysel is characterised by the typical cumulus orthopyroxene-dominated assemblage (Fig. 5).

The contamination of ultramafic magmas by carbonate lithologies promotes the overgrowth of Ca-rich phases, such as clinopyroxene and grossular garnet, over primary phases, such as orthopyroxene, and has been noted in several previous studies on mafic layered intrusions (Barnes et al., 2005; Iacono Marziano et al., 2008; Latypov et al., 2024). The crystallisation of Ca-rich plagioclase is also often evident (Chadwick et al., 2007) and where the footwall contains dolomite, magnesium-rich olivine is also commonly produced (Ganino et al., 2008). This trend is evident in this study through elevated *mg* values (Fig. 6), and previous studies on olivine mineral chemistry in the shallow Platreef at Sandsloot (Harris and Chaumba, 2001).

As well as assimilating dolomite upon emplacement, the Platreef magmas will have also interacted with CO_2, Ca and Mg-rich fluids which are released during the devolatilization of the footwall and incorporated xenoliths at Sandsloot. Mwenze et al. (2019) identified a skarn sequence at the contact between the Platreef and Malmani dolomite in one drillhole from Sandsloot, and argued that interactions with the Mg and Ca-rich footwall led to the formation of diopside and forsterite, producing Mg and Ca-rich (olivine-) clinopyroxenites. Although both the excess in Mg and Ca are thought to be sourced from the dolomite, they argue that the olivine clinopyroxenites only form distally to the Platreef intrusion, whereas the only clinopyroxenites form proximally, or within the Platreef intrusion. This is not the case in this study (Fig. 5). Nonetheless, the process of metasomatic interactions with the Malmani dolomite elevating the Ca and Mg contents of the Platreef magmas, altering the dominant mineral assemblage compared to elsewhere in the northern limb, and producing pegmatoidal textures (Fig. 2) is consistent with the observations in the current study, and has been reported in the genesis of skarns on the margins of ultramafic intrusions elsewhere (Mwenze et al., 2019; Wenzel et al., 2002). Mwenze et al. (2019) also reported the presence of prehnite as a key replacement mineral for plagioclase in the skarn sequence, which is also reflected in the deep Platreef at Sandsloot (Fig. 6).

5.2. Impact of footwall composition on PGE-Ni-Cu mineralisation in the Platreef

Several previous studies have noted the correlation between high grade PGE mineralisation and the Malmani dolomite footwall (Abernethy, 2019; De Waal, 1977; Holwell, 2006; Hutchinson and Kinnaird, 2005; Maier et al., 2008; McDonald and Holwell, 2011). This connection has been attributed to both primary magmatic and secondary hydrothermal processes linked to the Malmani dolomite, as well as pre-emplacement processes unrelated to carbonate contamination. The underlying mechanisms for why Sandsloot has some of the highest-grade material in the Platreef remains to be tested fully.

A key observation from this study is that where carbonate contamination is identified at Tweefontein (Figs. 4a-b, 5a-b and 6a-b), namely where the Penge and Duitschland forms the footwall, there is no increase in base or precious metal grade, however, at Sandsloot, where the Malmani dolomite forms the footwall, high-grade Ni-Cu-PGE mineralisation is found in strongly contaminated horizons. This may suggest that the carbonates present within the Malmani had a more profound effect on mineralisation than the Duitschland carbonates. The distinction between dolomitic versus carbonate contamination is indicated in the *mg* vs *si* diagram (Fig. 6), where the Platreef at Sandsloot is offset towards lower *si* and higher *mg* values, with the highest PGE grades found within this trend, indicated dolomitic contamination. At Tweefontein and

Overysel this trend is only present in minor intervals surrounded calc-silicate xenoliths. Although the Duitschland does contain horizons of dolomitized limestone, the majority of the carbonate succession is Mg-poor and therefore can be distinguished from the Malmani dolomite (Figs. 3 and 6). If dolomite contamination from the Malmani does play a role in elevating Ni-Cu-PGE grades, the lack of extensive dolomite within the country rocks at Tweefontein, may explain the lack of correlation between carbonate contamination and PGE-Ni-Cu grades there. The Duitschland also contains other units, such as shales, that may have counteracted or diluted any changes in $fO2$ caused by assimilating Duitschland carbonates.

Data from the Flatreef, the down-dip extension of the Platreef on the farm Turfspruit (Fig. 1) (Grobler et al., 2019; Keir-Sage et al., 2021; Maier et al., 2023; Maier et al., 2021), which intruded into Duitschland country rocks, is shown in Figure 7. There appears to be no clear trend between elevated carbonate contamination and elevated PGE grades (Fig. 7a-b) for this setting, with the majority of data clustered around orthopyroxenite compositions, including high grade intervals. Elevated Pt grades are present in some samples associated with carbonate contamination, with Niggli *c* values >20 and *si* values <100, however this association appears to be more random and far less systematic when compared to the data from Sandsloot (Figs. 4–6). The lower *si* values producing a downward trend in *si* vs *mg* space (Fig. 7c) can potentially be related to both elevated olivine (*si* = 50) abundance, as PGE-Ni-Cu mineralisation is often associated with harzburgite horizons in the Flatreef (Grobler et al., 2019; Maier et al., 2021), and carbonate contamination from the Duitschland. Few samples contain a corresponding increase in *mg* alongside the decrease in *si*, a key feature of the dolomite contaminated samples at Sandsloot (Fig. 6). Regardless, the majority of Flatreef data remains clustered on the pyroxene composition line (*si* = 100), and so no clear correlation can be made between contamination from the Duitschland and elevated PGE-Ni-Cu grades in the Flatreef. Maier et al. (2022) also found no link between PGE abundance and increased crustal contamination where mineralized intrusions were emplaced into the Duitschland footwall in the southern sector of the northern limb, a conclusion which is corroborated when examining the Niggli Numbers from the Flatreef (Fig. 8). This evidence further alludes to the potential importance of interactions with specifically the Malmani dolomite, as opposed to any carbonate sequence present within the Transvaal stratigraphy.

De Waal (1977) proposed that dolomitic contamination specifically is key to the formation of Ni-Cu-PGE deposits, arguing the addition of H_2O and CO_2 during the devolatilization of the country rock causes magma oxidation, which then triggers sulfide saturation. However, experimental studies have shown that the oxidation of basaltic magmas can actually stabilise sulfate, increasing the sulfur content at sulfide saturation (SCSS) of the magma, making it harder to reach sulfide saturation (Jugo, 2009; Jugo et al., 2005). It may therefore be the case that pre-emplacement contamination of a different crustal material in a deep-seated staging chamber was responsible for triggering sulfide saturation in this section of the Platreef. This model has been widely proposed for both the Platreef and UCZ of the eastern and western Bushveld (Eales and Costin, 2012; Maier et al., 2013; McDonald et al., 2009), with isotopic studies indicating both lower and upper crustal contaminants (Keet et al., 2023; Maier et al., 2000; Roelofse and Ashwal, 2012). Furthermore, with past studies reporting magmatic values for sulfides elsewhere in the Platreef (Holwell et al., 2007; Penniston-Dorland et al., 2008), crustal contamination is clearly not always required to trigger sulfide saturation.

Another key contrast between the three study locations is that PGE grades are significantly elevated at Sandsloot compared to both Tweefontein and Overysel (Fig. 4–6). In order to access the relationship between Ni-Cu-PGE grade, tenors and carbonate contamination, Cu/Pt is plotting against Niggli *c* in Figure 8. Pronost et al. (2008) alluded to the critical link between the Malmani dolomite and elevated PGE grades, suggesting that dolomite contamination plays a role in PGE

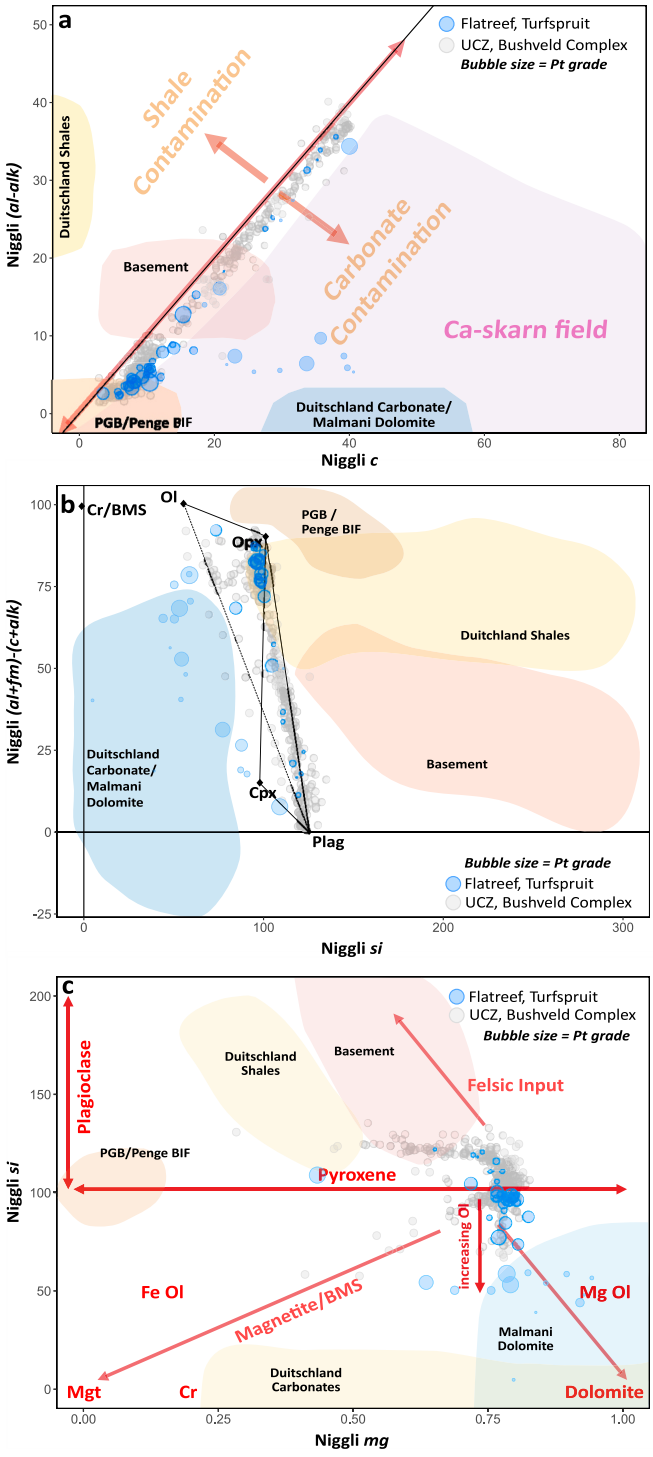

Fig. 7. Niggli Number plots for the Flatreef, Turfspruit, and the UCZ of the eastern and western limbs. For the Flatreef data the bubble size represents Pt grade; a) Niggli *(al-alk)* vs *c* bubble plot; b) Niggli *(al + fm)-(c + alk)* vs *si* bubble plot; c) Niggli *si* vs *mg* bubble plot. Flatreef data from Keir-Sage et al., 2021.

concentration and deposition. They suggested that the CO_2 produced during devolatilization of the footwall may enhance the PGE scavenging capacity of the sulfide liquid, thus increasing tenors of the sulfide minerals. The results in Figure 8 once again show that PGE grades are significantly elevated in the Platreef at Sandsloot, and that this is associated with elevated PGE tenors, inferred by the much lower Cu/Pt

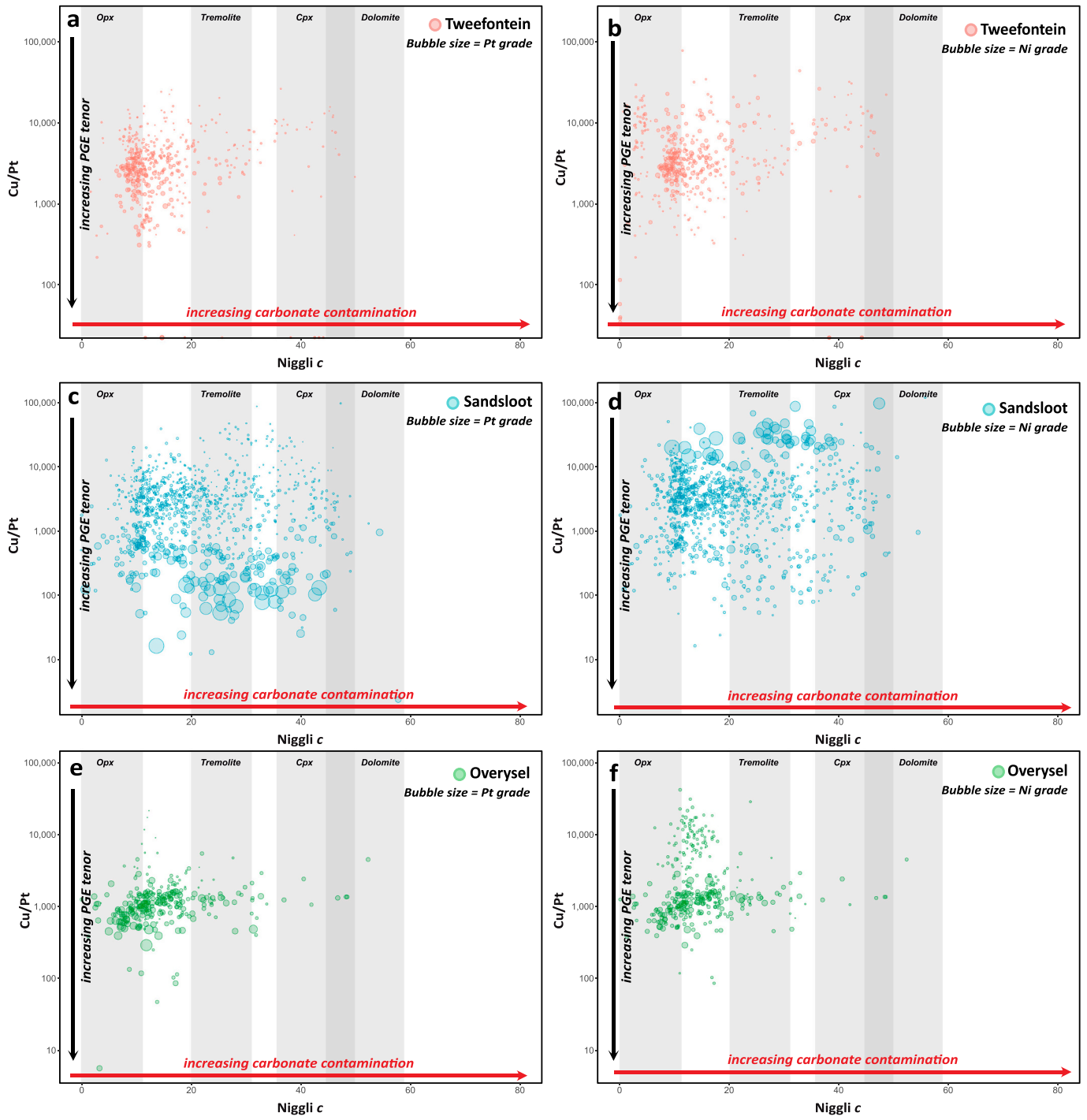

Fig. 8. Cu/Pt vs Niggli *c* for the Platreef at each study location. Mineral fields defined by their Niggli *c* compositions are from McDonald (2024). Bubble sizes for the Platreef data are scaled to either Pt (ppm) or Ni (wt%) grades; a-b) Tweefontein Pt and Ni grades respectively. Magmatic units only. No Ni data was available for drillholes TN303 or TN304; c-d) Sandsloot Pt and Ni grades respectively; e-f) Overysel Pt and Ni grades respectively.

values ($\leq$ 100, Fig. 8c). Nickel grades show an inverse relationship to PGE tenor, with the highest grades associated with much lower Cu/Pt ratios (Cu/Pt $\geq$ 10,000, Fig. 8d), which may be expected given these samples are associated with net-textured and massive sulfide mineralisation.

Whilst carbonate contamination is not always linked to Ni-Cu-PGE mineralisation within Sandsloot, when comparing between the three study locations it is clear that in the deep Platreef at Sandsloot both Ni-Cu-PGE grades and PGE tenors are significantly elevated compared to those locations which have not undergone considerable carbonate contamination from the Malmani dolomite (Fig. 8). Mechanisms by which interactions with the Malmani dolomite may have influenced PGE tenors at Sandsloot include increased rock-fluid interactions above the Malmani dolomite, allowing the remobilisation of PGEs at Sandsloot, potentially concentrating the PGEs at specific horizons in the Platreef stratigraphy, or influencing the PGE scavenging capacity of the sulfide liquid. Ongoing studies on silicate-hosted fluid inclusions from the Platreef revealed the presence of high temperature carbonate-dominated hypersaline brines (McFall et al., 2023). These Cl-rich brine inclusions, often associated with sulfide minerals, are proposed

to have been sourced from late magmatic degassing, or more likely, the devolatilization of the evaporite-bearing carbonate footwall, and may be capable of remobilising PGEs, Cu and Au in the Platreef (McFall et al., 2023). Should this be the case we might expect to see fractionation of Pd from Pt, due to its increased fluid mobility (Barnes and Liu, 2012), in these highly contaminated, fluid-altered zones. However, Pd/Pt ratios do not vary with Niggli *c* at Sandsloot (Fig. A7).

Alternatively, pre-emplacement processes, such as inherently more sulfide or PGE-fertile parental magmas, or S loss due to degassing (Iacono-Marziano et al., 2022), may have acted to increase the tenor of

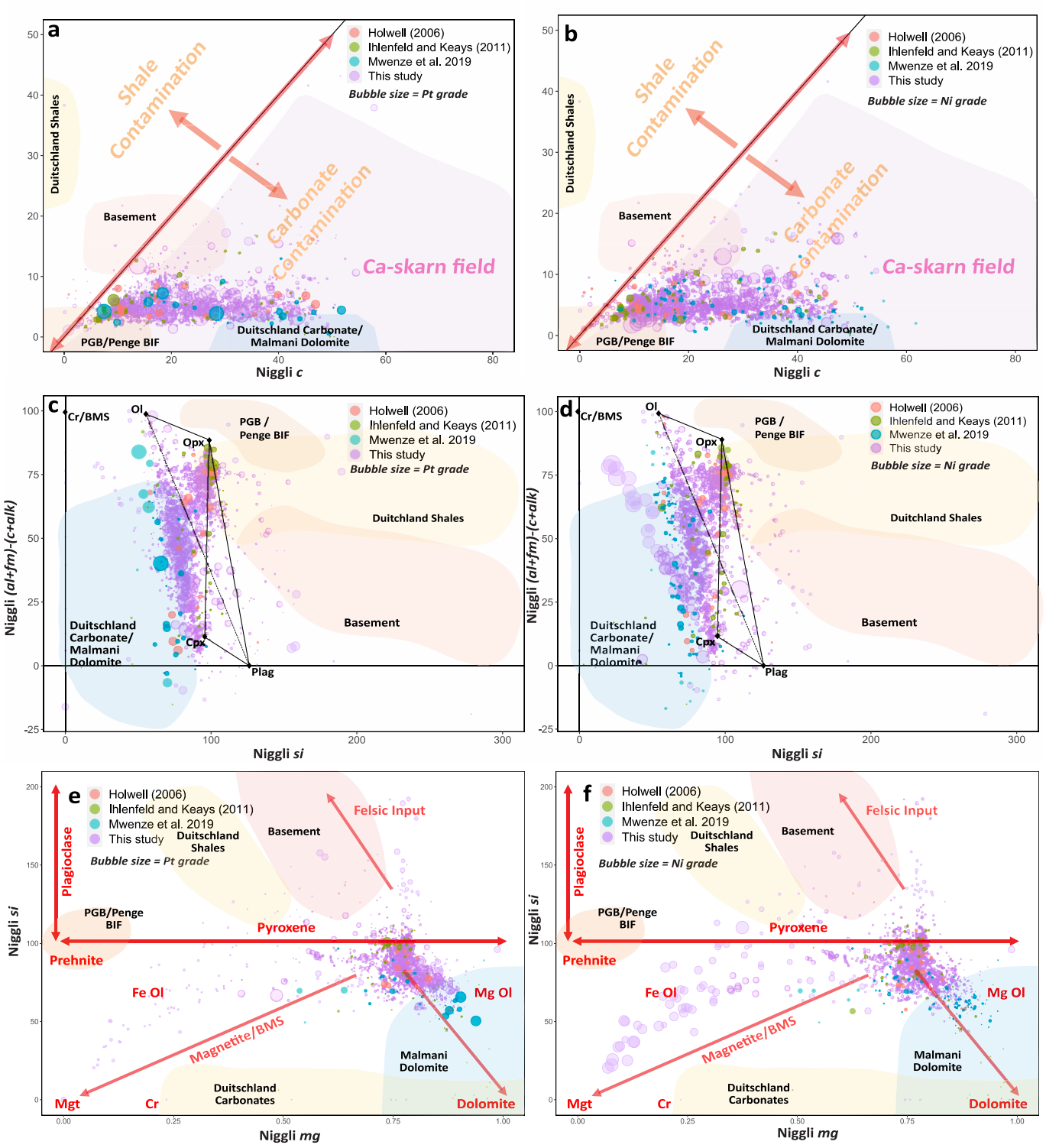

Fig. 9. Comparisons between the deeper Platreef at Sandsloot presented in this study, and previous studies from the shallower Platreef around the Mogalakwena pit at Sandsloot (Holwell, 2006; Ihlenfeld and Keays, 2011; Mwenze et al., 2019); a) Niggli *(al-alk)* vs *c* bubble plot. Bubble size corresponds to Pt (ppm) grade; b) Niggli *(al-alk)* vs *c* bubble plot. Bubble size corresponds to Ni (wt%) grade; c) Niggli *(al + fm)-(c + alk)* vs *si* bubble plot. Bubble size corresponds to Pt (ppm) grade; d) Niggli *(al + fm)-(c + alk)* vs *si* bubble plot. Bubble size corresponds to Ni (wt%) grades; e) Niggli *si* vs *mg* bubble plot. Bubble size corresponds to Pt (ppm) grades; f) Niggli *si* vs *mg* bubble plot. Bubble size corresponds to Ni (wt%) grades.

the sulfides at Sandsloot alone. The most likely of these processes is enhanced interactions of early formed sulfides with repeated magma pulses in a deeper staging chamber, a model which has been proposed for both the Platreef in general and Merensky Reef (Eales and Costin, 2012; McDonald et al., 2009; Naldrett et al., 2009). It may be possible that a staging chamber supplying the Platreef at Sandsloot alone allowed the upgrading of PGE tenors in sulfide which where then deposited in the deep Platreef at Sandsloot.

When comparing data from previous studies on the shallower Platreef at Sandsloot to the deeper Platreef sequence presented in this study (Fig. 9), both Pt and Ni grades are significantly elevated in the down-dip sequence. This may suggest that the Platreef magmas intruded into this deeper section were inherently more PGE-fertile upon emplacement due to the processes discussed above, or they have experienced enhanced interactions with the Malmani dolomite, which may have improved the PGE scavenging capabilities of the sulfide liquid, as supported by Pronost et al. (2008). It is worth noting here that the highest Pt grades identified by Mwenze et al. (2019) also trend strongly towards the dolomite contamination field (Fig. 9e). As outlined above, further analysis is required to fully constrain these processes and verify the contributions of dolomitic contamination.

Whereas the PGE-rich horizons at Sandsloot are not typically linked to increased sulfide abundance, Ni-rich samples are associated with net-textured and massive sulfide mineralisation (Fig. 2), which is not observed at Tweefontein and Overysel in this study. Other lenses of massive sulfide mineralisation have been discovered in the shallowest sections of the Platreef at Tweefontein (Nex, 2005), and at Turfspruit and Macalacaskop (Kinnaird et al., 2005) and these are often spatially associated with structural down-warps in the Transvaal footwall. Results from this study (Fig. 6) indicate that massive to semi-massive Ni mineralisation is associated with carbonate skarn minerals such a prehnite. Nickel-Cu-PGE mineralisation has been documented in skarn settings elsewhere, either associated with carbonate footwalls or calcsilicate xenoliths of varying scales (Lesher, 2017; Porter, 2016). However, massive sulfide mineralisation has not be reported in the shallow Platreef at Sandsloot (Fig. 4) (Armitage et al., 2002; Holwell, 2006; Ihlenfeld and Keays, 2011; McDonald et al., 2005), even when skarn sequences have been identified, such as by Mwenze et al. (2019). The skarn related samples in this study (shown in blue in Fig. 9) instead show elevated Pt contents, as opposed to Ni in the deeper drillholes included in this study.

The Malmani dolomite forms the host rock to another significant Ni-sulfide deposit in South Africa: the Nkomati deposit in the Uitkomst Intrusion to the east of the Bushveld Complex. Maier et al. (2018) proposed a mechanism for the magmatic erosion of the dolomite footwall here, leading to the creation of a *syn*-emplacement down-warp structure, followed by the slumping and accumulation of sulfide and chromite-rich slurries within the partially eroded dolomite. This model suggests that the Malmani dolomite may be more easily eroded by mafic magmas than the carbonaceous shale successions within the Duitschland, with the devolatilization process resulting in a loss of mass in the dolomite, creating a trough structure, further promoting magma erosion. We suggest that this process may have occurred locally at Sandsloot, and led to the accumulation of the massive sulfide lens intersected by SSAA019, and associated enhanced Ni—Cu grades. Additionally, the location of this study area on the northern side of the prominent Transvaal anticline structure, known as the Dolomite Tongue (Fig. 1), thought to be a pre-Bushveld deformation structure (Armitage, 2011), has likely aided the slumping and accumulation of sulfide liquid. Fluids produced via the devolatilization of calcareous sediments has also been proposed to aid the downward percolation of sulfides, which may further aid this slumping process (Abernethy, 2019; Maier et al., 2021). Why this massive sulfide lens is not more pervasive across the suite of drillholes studied at Sandsloot is difficult to constrain, but is likely due to the structure or topography of the footwall (either pre-emplacement or due to differences in magmatic erosion).

Although there is clearly a strong correlation between increased Ni-Cu-PGE mineralisation and carbonate contamination from the Malmani dolomite at Sandsloot, with the highest grades only present above this footwall unit, the degree to which this contamination has acted directly to increase PGE tenors and grades requires further testing. It remains possible that pre-emplacement processes, such as those in deeper staging chambers as discussed above, acted to enhance Ni-Cu-PGE grades at Sandsloot before interactions with the Malmani dolomite. However, the link between carbonate, and specifically dolomitic, contamination in the genesis of this world-class PGE-Ni-Cu deposit, is noteworthy and presents an intriguing question on localised controls on upgrading world class mineralisation, and that practically, this can be identified simply and easily using Niggli numbers.

6. Conclusions

The intrusion of the Platreef over the sediments of the Transvaal Supergroup makes it a much more dynamic and heterogeneous system compared to the CZ of the eastern and western limbs, with significant variations in both the degree and style of mineralisation observed. Niggli Numbers are shown to be an effective tool for quickly and effectively characterising these variations using data from igneous and hybrid/sedimentary lithologies, as well as allowing the potential controls on PGE-Ni-Cu mineralisation to be scrutinised. This application has great potential as it utilises whole rock major element data and therefore access to a large database including historic data sets opening the opportunity to develop machine learning algorithms and techniques to detect and define patterns or evolutionary trends.

This study supports previous work showing that carbonate contamination from the underlying Malmani dolomite is correlated to significant PGE-Ni-Cu mineralisation at Sandsloot. At Tweefontein and Overysel, local contamination does not exhibit a strong relationship the degree of mineralisation, with the highest-grade horizons associated with the least contamination from both carbonate and granitic sources. Furthermore, both PGE and Ni grades are significantly enhanced at Sandsloot compared to the other study areas, as well as the shallower Platreef previously studied at Sandsloot.

Although Niggli Numbers alone are not able to verify the processes by which contamination from the Malamani dolomite may lead to elevated Ni-Cu-PGE grades at Sandsloot, and other pre-emplacement models for enhancing Ni-Cu-PGE grades remain possible, this study highlights clearly a key distinction from the Platreef at Sandsloot compared to Tweefontein and Overysel. This clearly warrants further study given the highest grades of one of the world's largest PGE-Ni-Cu deposits are located here.

CRediT authorship contribution statement

Erin S. Thompson: Writing – review & editing, Writing – original draft, Investigation, Formal analysis, Data curation, Conceptualization. **David A. Holwell:** Writing – review & editing, Validation, Supervision, Funding acquisition, Conceptualization. **Iain McDonald:** Writing – review & editing, Supervision, Methodology, Funding acquisition, Conceptualization. **Marc Reichow:** Writing – review & editing, Supervision. **Thomas G. Blenkinsop:** Writing – review & editing, Supervision, Funding acquisition. **Hannah S.R. Hughes:** Supervision, Funding acquisition. **Katie McFall:** Writing – review & editing, Supervision. **Kate R. Canham:** Writing – review & editing, Validation. **Matthew A. Loader:** Writing – review & editing, Supervision. **Lara Du Preez:** Supervision, Data curation. **Kofi Acheampong:** Supervision, Data curation. **Andy Lloyd:** Supervision, Funding acquisition, Conceptualization.

Declaration of competing interest

The authors declare that they have no known competing financial interests or personal relationships that could have appeared to influence

the work reported in this paper.

Data availability

The data presented in this paper was supplied by Anglo American as part of the Northern Limb in 4D (NL4D) research consortium, and is therefore not available in its raw format due to its commercially sensitive nature.

Acknowledgements

The study was funded by Anglo American as part of the NL4D (Northern Limb in 4D) research consortium, and awarded to the University of Leicester, Cardiff University and Camborne School of Mines at the University of Exeter. The authors wish to thank Anglo American for access to their data from the study location, and samples which were analysed as part of the study. Thin sections were made at the University of Leicester by Dr. Annika Burns, and thanks is also given to Lin Marvin for their help during XRF analysis at the University of Leicester. For the purposes of open access, the author has applied a creative commons attribution (CC BY) licence to any Author Accepted Manuscript version arising from this submission.

Appendix A. Supplementary data

Supplementary data to this article can be found online at https://doi.org/10.1016/j.chemgeo.2024.122481.

References

Abernethy, K.E.L., 2019. Assimilation of Dolomite by Bushveld Magmas in the Flatreef; Implications for the Origin of Ni-cu-PGE Mineralization and the Precambrian Atmosphere (PhD Thesis).. Cardiff University.

Aitchison, J., 1984. The statistical analysis of geochemical compositions. Math. Geol. 16, 531–564. https://doi.org/10.1007/BF01029316.

Armitage, P.E.B., 2011. Development of the Platreef in the Northern Limb of the Bushveld Complex at Sandsloot, Mokopane District, South Africa. University of Greenwich.

Armitage, P.E.B., McDonald, Iain, Edwards, S.J., Manby, G.M., 2002. Platinum-group element mineralization in the Platreef and calc-silicate footwall at Sandsloot, Potgietersrus District, South Africa. Trans. Instit. Min. Metall. Sect. B Appl. Earth Sci. 111.

Barnes, S.J., Liu, W., 2012. Pt and Pd mobility in hydrothermal fluids: evidence from komatiites and from thermodynamic modelling. Ore Geol. Rev. 44, 49–58. https://doi.org/10.1016/j.oregeorev.2011.08.004.

Barnes, C.G., Prestvik, T., Sundvoll, B., Surratt, D., 2005. Pervasive assimilation of carbonate and silicate rocks in the Hortavær igneous complex, north-Central Norway. Lithos Granit. Syst. 80, 179–199. https://doi.org/10.1016/j.lithos.2003.11.002.

Barton, J.M., Cawthorn, R.G., White, J., 1986. The role of contamination in the evolution of the platreef of the Bushveld complex. Econ. Geol. 81, 1096–1104.

Blanks, D.E., Holwell, D.A., Barnes, S.J., Boyce, A.J., 2019. Unravelling the dynamic emplacement of the carbonate-rich Munali Ni–Cu–PGE breccia deposit, Zambia. Appl. Earth Sci. 128, 39–40. https://doi.org/10.1080/25726838.2019.1599203.

Blanks, D.E., Holwell, D.A., Barnes, S.J., Schoneveld, L.E., Boyce, A.J., Mbiri, L., 2022. Evolution of the Munali Intrusive complex: host to a carbonate-rich Ni-(Cu-PGE) sulfide deposit. Ore Geol. Rev. 150, 105109. https://doi.org/10.1016/j.oregeorev.2022.105109.

Buccianti, A., Grunsky, E., 2014. Compositional data analysis in geochemistry: are we sure to see what really occurs during natural processes? J. Geochem. Explor. Compos. 141, 1–5. https://doi.org/10.1016/j.gexplo.2014.03.022.

Buchanan, D.L., Rouse, J.E., 1984. Role of contamination in the precipitation of sulphides in the Platreef of the Bushveld complex. In: Presented at the Nickel Sulphide Field Conference, 3, pp. 141–146.

Buchanan, D.L., Nolan, J., Suddaby, P., Rouse, J.E., Viljoen, M.J., Davenport, J.W.J., 1981. The genesis of sulfide mineralization in a portion of the Potgietersrus limb of the Bushveld complex. Econ. Geol. 76, 568–579. https://doi.org/10.2113/gsecongeo.76.3.568.

Cawthorn, R.G., Barton, J.M., Viljoen, M.J., 1985. Interaction of floor rocks with the Platreef on Overysel, Potgietersrus, northern Transvaal. Econ. Geol. 80, 988–1006. https://doi.org/10.2113/gsecongeo.80.4.988.

Chadwick, J.P., Troll, V.R., Ginibre, C., Morgan, D., Gertisser, R., Waight, T.E., Davidson, J.P., 2007. Carbonate assimilation at Merapi Volcano, Java, Indonesia: insights from crystal isotope stratigraphy. J. Petrol. 48, 1793–1812. https://doi.org/10.1093/petrology/egm038.

De Waal, S.A., 1977. Carbon dioxide and water from metamorphic reactions as agents for sulphide and spinel precipitation in mafic magmas. Trans. Geol. Soc. S. Afr. 80, 193–196.

de Wit, M.J., 1991. Archaean greenstone belt tectonism and basin development: some insights from the Barberton and Pietersburg greenstone belts, Kaapvaal Craton, South Africa. J. Afr. Earth Sci. 13, 45–63. https://doi.org/10.1016/0899-5362(91)90043-X.

Eales, H.V., Cawthorn, R.G., 1996. The Bushveld complex. Dev. Petrol. 15, 181–229. https://doi.org/10.1016/S0167-2894(96)80008-X.

Eales, H.V., Costin, G., 2012. Crustally contaminated komatiite: primary source of the chromitites and marginal, lower, and critical zone magmas in a staging chamber beneath the Bushveld complex. Econ. Geol. 107, 645–665. https://doi.org/10.2113/econgeo.107.4.645.

Gain, S.B., Mostert, A.B., 1982. The geological setting of the platinoid and base metal sulfide mineralization in the Platreef of the Bushveld complex in Drenthe, North of Potgietersrus. Econ. Geol. 77, 1395–1404. https://doi.org/10.2113/gsecongeo.77.6.1395.

Ganino, C., Arndt, N.T., Zhou, M.-F., Gaillard, F., Chauvel, C., 2008. Interaction of magma with sedimentary wall rock and magnetite ore genesis in the Panzhihua mafic intrusion, SW China. Mineral. Deposita 43, 677–694. https://doi.org/10.1007/s00126-008-0191-5.

Grobler, D.F., Brits, J.A.N., Maier, W.D., Crossingham, A., 2019. Litho- and chemostratigraphy of the Flatreef PGE deposit, northern Bushveld complex. Mineral. Deposita 54, 3–28. https://doi.org/10.1007/s00126-018-0800-x.

Harris, C., Chaumba, J.B., 2001. Crustal contamination and fluid-rock interaction during the formation of the Platreef, northern limb of the Bushveld complex, South Africa. J. Petrol. 42, 1321–1347. https://doi.org/10.1093/petrology/42.7.1321.

Holwell, D.A., 2006. The Roles of Magmatism, Contamination and Hydrothermal Processes in the Development of the Platreef Mineralization, Bushveld Complex, South Africa. Cardiff University.

Holwell, D.A., Jordaan, A., 2006. Three-dimensional mapping of the Platreef at the Zwartfontein South mine: implications for the timing of magmatic events in the northern limb of the Bushveld complex, South Africa. Trans. Instit. Mining Metall. Sect. B Appl. Earth Sci. 115, 41–48. https://doi.org/10.1179/174327506X113046.

Holwell, D.A., McDonald, I., 2006. Petrology, geochemistry and the mechanisms determining the distribution of platinum-group element and base metal sulphide mineralisation in the Platreef at Overysel, northern Bushveld complex, South Africa. Mineral. Deposita 41, 575–598. https://doi.org/10.1007/s00126-006-0083-5.

Holwell, D.A., Armitage, P.E.B., McDonald, I., 2005. Observations on the relationship between the Platreef and its hangingwall. Trans. Instit. Mining Metall. Sect. B Appl. Earth Sci. 114. https://doi.org/10.1179/037174505X62875.

Holwell, D.A., McDonald, I., Armitage, P.E.B., 2006. Platinum-group mineral assemblages in the Platreef at the Sandsloot Mine, northern Bushveld complex, South Africa. Mineral. Mag. 70, 83–101. https://doi.org/10.1180/0026461067010315.

Holwell, D.A., Boyce, A.J., McDonald, I., 2007. Sulfur isotope variations within the Platreef Ni-Cu-PGE deposit: genetic implications for the origin of sulfide mineralization. Econ. Geol. 102, 1091–1110.

Hutchinson, D., Kinnaird, J.A., 2005. Complex multistage genesis for the Ni–Cu–PGE mineralisation in the southern region of the Platreef, Bushveld complex, South Africa. Appl. Earth Sci. 114, 208–224. https://doi.org/10.1179/037174505X82125.

Iacono Marziano, G., Gaillard, F., Pichavant, M., 2008. Limestone assimilation by basaltic magmas: an experimental re-assessment and application to Italian volcanoes. Contrib. Mineral. Petrol. 155, 719–738. https://doi.org/10.1007/s00410-007-0267-8.

Iacono-Marziano, G., Le Vaillant, M., Godel, B.M., Barnes, S.J., Arbaret, L., 2022. The critical role of magma degassing in sulphide melt mobility and metal enrichment. Nat. Commun. 13, 2359. https://doi.org/10.1038/s41467-022-30107-y.

Ihlenfeld, C., Keays, R.R., 2011. Crustal contamination and PGE mineralization in the Platreef, Bushveld complex, South Africa: evidence for multiple contamination events and transport of magmatic sulfides. Mineral. Deposita 46, 813–832. https://doi.org/10.1007/s00126-011-0340-0.

Jowitt, S.M., Keays, R.R., 2011. Shale-hosted Ni–(Cu–PGE) mineralisation: a global overview. Appl. Earth Sci. 120, 187–197. https://doi.org/10.1179/1743275812Z.00000000026.

Jugo, P.J., 2009. Sulfur content at sulfide saturation in oxidized magmas. Geology 37, 415–418. https://doi.org/10.1130/G25527A.1.

Jugo, P.J., Luth, R.W., Richards, J.P., 2005. An experimental study of the sulfur content in basaltic melts saturated with immiscible sulfide or sulfate liquids at 1300°C and 1·0 GPa. J. Petrol. 46, 783–798. https://doi.org/10.1093/petrology/egh097.

Keays, R.R., 1995. The role of komatiitic and picritic magmatism and S-saturation in the formation of ore deposits. Lithos 34, 1–18. https://doi.org/10.1016/0024-4937(95)90003-9.

Keet, J.J., Roelofse, F., Gauert, C.D.K., Iaccheri, L.M., Grobler, D.F., Ueckermann, H., 2023. Neodymium Isotope Variations in the Flatreef on Macalacaskop, Northern Limb, Bushveld Complex. Miner Deposita. https://doi.org/10.1007/s00126-023-01202-x.

Keir-Sage, E., Leybourne, M.I., Jugo, P.J., Grobler, D.F., Mayer, C.C., 2021. Assessing the extent of local crust assimilation within the Flatreef, northern limb of the Bushveld Igneous complex, using sulfur isotopes and trace element geochemistry. Mineral. Deposita 56, 91–102. https://doi.org/10.1007/s00126-020-01024-1.

Kinnaird, J.A., 2005. Geochemical evidence for multiphase emplacement in the southern Platreef. Trans. Instit. Mining Metall. Sect. B Appl. Earth Sci. 114. https://doi.org/10.1179/037174505X82152.

Kinnaird, J.A., McDonald, I., 2005. An introduction to mineralisation in the northern limb of the Bushveld complex. Trans. Instit. Mining Metall. Sect. B Appl. Earth Sci. 114. https://doi.org/10.1179/037174505X62893.

Kinnaird, J.A., Hutchinson, D., Schurmann, L., Nex, P.A.M., de Lange, R., 2005. Petrology and mineralisation of the southern Platreef: Northern limb of the Bushveld complex, South Africa. Mineral. Deposita 40, 576–597. https://doi.org/10.1007/s00126-005-0023-9.

Krivolutskaya, N.A., Plechova, A.A., Kostitsyn, Yu.A., Belyatsky, B.V., Roshchina, I.A., Svirskaya, N.M., Kononkova, N.N., 2014. Geochemical aspects of the assimilation of host rocks by basaltic magmas during the formation of Noril'sk Cu-Ni ores. Petrology 22, 128–150. https://doi.org/10.1134/S0869591114020052.

Latypov, R.M., Namur, O., Bai, Y., Barnes, S.-J., Chistyakova, Sy, Holness, M.B., Iacono-Marziano, G., Kruger, W.A.J., O'Driscoll, B., Smith, W.D., Virtanen, V.J., Wang, C.Y., Xing, C.-M., Charlier, B., 2024. Layered intrusions: fundamentals, novel observations and concepts, and controversial issues. Earth Sci. Rev. 249, 104653. https://doi.org/10.1016/j.earscirev.2023.104653.

Lehmann, J., Arndt, N., Windley, B., Zhou, M.-F., Wang, C.Y., Harris, C., 2007. Field relationships and geochemical constraints on the emplacement of the Jinchuan intrusion and its Ni-Cu-PGE sulfide deposit, Gansu, China. Econ. Geol. 102, 75–94. https://doi.org/10.2113/gsecongeo.102.1.75.

Lesher, C.M., 2017. Roles of xenomelts, xenoliths, xenocrysts, xenovolatiles, residues, and skarns in the genesis, transport, and localization of magmatic Fe-Ni-Cu-PGE sulfides and chromite. Ore Geol. Rev. 90, 465–484. https://doi.org/10.1016/j.oregeorev.2017.08.008.

Lightfoot, P.C., Keays, R.R., Evans-Lamswood, D., Wheeler, R., 2012. S saturation history of Nain Plutonic Suite mafic intrusions: origin of the Voisey's Bay Ni–Cu–Co sulfide deposit, Labrador, Canada. Mineral. Deposita 47, 23–50. https://doi.org/10.1007/s00126-011-0347-6.

Maier, W.D., Arndt, N.T., Curl, E.A., 2000. Progressive crustal contamination of the Bushveld complex: evidence from Nd isotopic analyses of the cumulate rocks. Contrib. Mineral. Petrol. 140, 316–327. https://doi.org/10.1007/s004100000186.

Maier, W.D., de Klerk, L., Blaine, J., Manyeruke, T., Barnes, S.J., Stevens, M.V.A., Mavrogenes, J.A., 2008. Petrogenesis of contact-style PGE mineralization in the northern lobe of the Bushveld complex: comparison of data from the farms Rooipoort, Townlands, Drenthe and Nonnenwerth. Mineral. Deposita 43, 255–280. https://doi.org/10.1007/s00126-007-0145-3.

Maier, W.D., Barnes, S.J., Groves, D.I., 2013. The Bushveld complex, South Africa: Formation of platinum-palladium, chrome- and vanadium-rich layers via hydrodynamic sorting of a mobilized cumulate slurry in a large, relatively slowly cooling, subsiding magma chamber. Mineral. Deposita 48, 1–56. https://doi.org/10.1007/s00126-012-0436-1.

Maier, W.D., Abernethy, K.E.L., Grobler, D.F., Moorhead, G., 2021. Formation of the Flatreef deposit, northern Bushveld, by hydrodynamic and hydromagmatic processes. Mineral. Deposita 56, 11–30. https://doi.org/10.1007/s00126-020-00987-5.

Maier, W.D., Brits, A., Grobler, D., 2022. Petrogenesis of PGE mineralised intrusions in the floor of the northern Bushveld Complex. S. Afr. J. Geol. 2022 125 (3–4), 265–290.

Maier, W.D., Barnes, S.J., Godel, B.M., Grobler, D., Smith, W.D., 2023. Petrogenesis of thick, high-grade PGE mineralisation in the Flatreef, northern Bushveld complex. Mineral. Deposita. https://doi.org/10.1007/s00126-022-01156-6.

Maier, W.D., Prevec, S.A., Scoates, J.S., Wall, C.J., Barnes, S.J., Gomwe, T., 2018. The Uitkomst intrusion and Nkomati Ni-Cu-Cr-PGE deposit, South Africa: trace element geochemistry, Nd isotopes and high-precision geochronology. Miner. Deposita 53, 67–88.

Manyeruke, T.D., Maier, W.D., Barnes, S.-J., 2005. Major and trace element geochemistry of the Platreef on the farm Townlands, northern Bushveld complex. S. Afr. J. Geol. 108, 381–396.

McCutcheon, S., 2012. Platinum-Group Mineral Assemblages in the Platreef on Tweefontein, Northern Bushveld Complex, South Africa (MSc). University of Witwatersrand.

McDonald, I., 2024. Reimagining Niggli Numbers for modern data applications in petrology and exploration geochemistry. Chem. Geol. 650, 121915. https://doi.org/10.1016/j.chemgeo.2023.121915.

McDonald, I., Holwell, D.A., 2011. Geology of the Northern Bushveld complex and the setting and Genesis of the Platreef Ni-Cu-PGE Deposit. Rev. Econ. Geol. Soc. Econ. Geol. https://doi.org/10.5382/rev.17.11.

McDonald, I., Holwell, D.A., Armitage, P.E.B., 2005. Geochemistry and mineralogy of the Platreef and "critical Zone" of the northern lobe of the Bushveld complex, South Africa: implications for Bushveld stratigraphy and the development of PGE mineralisation. Mineral. Deposita 40, 526–549. https://doi.org/10.1007/s00126-005-0018-6.

McDonald, I., Holwell, D.A., Wesley, B., 2009. Assessing the potential involvement of an early magma staging chamber in the generation of the Platreef Ni-Cu-PGE deposit in the northern limb of the Bushveld complex: a pilot study of the lower Zone complex at Zwartfontein. Trans. Instit. Mining Metall. Sect. B Appl. Earth Sci. 118, 5–20. https://doi.org/10.1179/174327509X434902.

McFall, K., McDonald, I., Hanley, J.J., Kerr, M., Yudovskaya, M.A., Kinnaird, J., Tattitch, B., 2023. Carbonate-dominated hypersaline brines in the northern Bushveld complex and their role in metal transport. In: Abstracts from the 14th International Platinum Symposium and the Wager & Brown Workshop Technical Session. Presented at the 14th International Platinum Symposium, the Canadian Journal of Mineralogy and Petrology. Cardiff University, pp. 1421–1423.

Muthuswami, T.N., 1952. Niggli's principles of Igneous petrogenesis. In: Proceedings of the Indian Academy of Sciences, section a. Indian Academy of Sciences, pp. 1–40.

Mwenze, T., Okujeni, C., Frei, D., Siad, A., Bailie, R., 2019. Geochemical controls on the distribution of PGE mineralisation in skarns formed during emplacement of the Platreef in the Northern limb of the Bushveld complex, South Africa. J. Geochem. Explor. 205. https://doi.org/10.1016/j.gexplo.2019.106340.

Naldrett, A.J., 1992. A model for the Ni-Cu-PGE ores of the Noril'sk region and its application to other areas of flood basalt. Econ. Geol. 87, 1945–1962. https://doi.org/10.2113/gsecongeo.87.8.1945.

Naldrett, A.J., 2005. A history of our understanding of magmatic Ni-Cu sulfide deposits. Can. Mineral. 43, 2069–2098. https://doi.org/10.2113/gscanmin.43.6.2069.

Naldrett, A.J., Wilson, A., Kinnaird, J., Chunnett, G., 2009. PGE tenor and metal ratios within and below the Merensky Reef, Bushveld complex: implications for its genesis. J. Petrol. 50, 625–659. https://doi.org/10.1093/petrology/egp015.

Nex, P.A.M., 2005. The structural setting of mineralisation on Tweefontein Hill, northern limb of the Bushveld complex, South Africa. Trans. Instit. Mining Metall. Sect. B Appl. Earth Sci. 114. https://doi.org/10.1179/037174505X62901.

Niggli, P., 1954. Rocks and Mineral Deposits. W.H. Freeman and Co., San Francisco.

Nyama, Nesbert, Nex, P.A.M., Nyama, N., Nex, P., Yao, Y., 2005. Preliminary petrological studies of the platreef on Tweefontein Hill, bushveld igneous complex, South Africa. In: 10th International Platinum Symposium.

Pearce, T.H., 1968. A contribution to the theory of variation diagrams. Contrib. Mineral. Petrol. 19, 142–157. https://doi.org/10.1007/BF00635485.

Penniston-Dorland, S.C., Wing, B.A., Nex, P.A.M., Kinnaird, J.A., Farquhar, J., Brown, M., Sharman, E.R., 2008. Multiple sulfur isotopes reveal a magmatic origin for the Platreef platinum group element deposit, Bushveld complex, South Africa. Geology 36, 979–982. https://doi.org/10.1130/G25098A.1.

Porter, T.M., 2016. Regional tectonics, geology, magma chamber processes and mineralisation of the Jinchuan nickel-copper-PGE deposit, Gansu Province, China: a review. Geosci. Front. 7, 431–451. https://doi.org/10.1016/j.gsf.2015.10.005. Special Issue: Giant Mineral Deposits.

Pronost, J., Harris, C., Pin, C., 2008. Relationship between footwall composition, crustal contamination, and fluid–rock interaction in the Platreef, Bushveld complex, South Africa. Mineral. Deposita 43, 825–848. https://doi.org/10.1007/s00126-008-0203-5.

Roelofse, F., Ashwal, L.D., 2012. The lower Main Zone in the Northern Limb of the Bushveld Complex-a >1·3 km thick sequence of intruded and variably contaminated crystal mushes. J. Petrol. 53, 1449–1476. https://doi.org/10.1093/petrology/egs022.

Scoon, R.N., Costin, G., Mitchell, A.A., Moine, B., 2020. Non-sequential injection of PGE-rich ultramafic sills in the platreef unit at akanani, northern limb of the bushveld complex: evidence from Sr and Nd isotopic systematics. J. Petrol. 61. https://doi.org/10.1093/petrology/egaa032.

Seat, Z., Beresford, S.W., Grguric, B.A., Gee, M.A.M., Grassineau, N.V., 2009. Reevaluation of the role of external sulfur addition in the genesis of Ni-Cu-PGE deposits: evidence from the Nebo-Babel Ni-Cu-PGE Deposit, West Musgrave, Western Australia. Econ. Geol. 104, 521–538. https://doi.org/10.2113/gsecongeo.104.4.521.

Sharman, E.R., Penniston-Dorland, S.C., Kinnaird, J.A., Nex, P.A.M., Brown, M., Wing, B. A., 2013. Primary origin of marginal Ni-Cu-(PGE) mineralization in layered intrusions: δ33s evidence from the Platreef, Bushveld, South Africa. Econ. Geol. 108, 365–377. https://doi.org/10.2113/econgeo.108.2.365.

Sharman-Harris, E.R., Kinnaird, J.A., Harris, C., Horstmann, U.E., 2005. A new look at sulphide mineralisation of the northern limb, Bushveld complex: a stable isotope study. Appl. Earth Sci. 114, 252–263. https://doi.org/10.1179/037174505X82134.

Sluzhenikin, S.F., Malitch, K.N., Yudovskaya, M.A., Turovtsev, D.M., Antsiferova, T.N., Mikhalev, S.K., Badanina, I.Yu., Soloshenko, N.G., 2023. Lower talnakh type intrusions of the Norilsk Ore Region. Petrology 31, 492–518. https://doi.org/10.1134/S0869591123050065.

Stephenson, H., 2018. The Platreef Magma Event at the World-Class Turfspruit Ni-cu-PGE Deposit: Implications for Mineralisation Processes and the Bushveld Complex Stratigraphy (PhD Thesis).. Cardiff University.

Toens, P.D., 1954. Hybrid Rocks in the Floor of the Bushveld Complex. Transactions of the Geological Society of South Africa.

Wenzel, T., Baumgartner, L.P., Brugmann, G.E., Konnikov, E.G., Kislov, E.V., 2002. Partial melting and assimilation of dolomitic xenoliths by mafic magma: the Ioko-Dovyren Intrusion (North Baikal Region, Russia). J. Petrol. 43, 2049–2074. https://doi.org/10.1093/petrology/43.11.2049.

White, J.A., 1994. The Potgietersrus prospect—geology and exploration history. In: Proceedings of the 15th Congress of the Council of Metallurgical and Mining Institutions, Volume 3, 14. Presented at the South African Institute of Mining and Metallurgy Symposium Series, pp. 173–181.

Yang, Z.-F., Li, J., Jiang, Q.-B., Xu, F., Guo, S.-Y., Li, Y., Zhang, J., 2019. Using major element logratios to recognize compositional patterns of basalt: implications for source lithological and compositional heterogeneities. J. Geophys. Res. Solid Earth 124, 3458–3490. https://doi.org/10.1029/2018JB016145.

Yudovskaya, M., Kinnaird, J., Naldrett, A.J., Mokhov, A.V., Mcdonald, I., Reinke, C., 2011. Facies variation in PGE mineralization in the Central Platreef of the Bushveld complex, South Africa. Can. Mineral. 49, 1349–1384. https://doi.org/10.3749/canmin.49.6.1349.